Mechanisms of Thermal Quenching of Defect-related Luminescence in Semiconductors

Michael A. Reshchikov[1]

Department of Physics, Virginia Commonwealth University, Richmond, VA 23220, USA

ABSTRACT

The intensity of defect-related photoluminescence (PL) in semiconductors changes with temperature, and it usually decreases exponentially above some critical temperature, a process called the PL quenching. Here, main mechanisms of PL quenching are reviewed. Most examples are given for defects in GaN as the most studied modern semiconductor, which has important applications in technology. Peculiarities of defect-related PL in I-VII, II-VI and III-V compounds are also reviewed. We distinguish three basic mechanisms of PL quenching. Most examples of PL quenching can be explained by the Schön-Klasens mechanism, whereas very few or even no confirmed cases can be found in support of the Seitz-Mott mechanism. Third mechanism, the abrupt and tunable quenching, is common for high-resistivity semiconductors. Temperature dependence of capture coefficients and a number of other reasons may affect the temperature dependence of PL intensity. The "negative quenching" or a significant rise of PL intensity with temperature is explained by a competition between recombination channels for minority carriers.

[1] Prof. M. A. Reshchikov
Department of Physics
Virginia Commonwealth University
701 West Grace St., Richmond, VA 23220, U.S.A.
E-mail: *mreshchi@vcu.edu*

This article has been accepted for publication and undergone full peer review but has not been through the copyediting, typesetting, pagination and proofreading process, which may lead to differences between this version and the Version of Record. Please cite this article as doi: 10.1002/pssa.202000101

1. Introduction

Photoluminescence (PL) is a powerful tool to study point defects in semiconductors. Point defects are native defects, impurities and various complexes, while semiconductors in general include also insulating crystals with wide bandgap. Shape and intensity of defect-related PL bands may change significantly with variation of temperature. The PL intensity, I^{PL}, commonly decreases exponentially with increasing temperature above a characteristic temperature T_0, a process called the PL quenching. The following empirical formula is universally used to fit the $I^{PL}(T)$ dependence:

$$I^{PL}(T) = \frac{I^{PL}(0)}{1 + C \exp\left(-\frac{E_A}{kT}\right)}, \qquad (1)$$

where C is a constant, E_A is some activation energy, and k is Boltzmann's constant.[1] Although there is a consensus on applicability of Equation (1) to PL from point defects, the interpretation of PL quenching in semiconductors is often controversial and confusing.[2]

According to one model (Seitz-Mott or one-center mechanism),[3,4] the PL quenching is caused by a gradual replacement of radiative transitions with non-radiative ones in the same defect. This mechanism can be explained by invoking the configuration coordinate model (**Figure 1**).[5,6] The slope of the $I^{PL}(T)$ dependence at $T > T_0$ in the Arrhenius plot reveals an activation energy, which is equal to the energy difference between the potential minimum of the excited state and the cross-over point of the excited and ground states of the defect ($E_A = E_2$). As for the coefficient C, it is equal to the product of PL lifetime in the excited state and the vibrational frequency of the defect (on the order of 10^{13} s^{-1}).

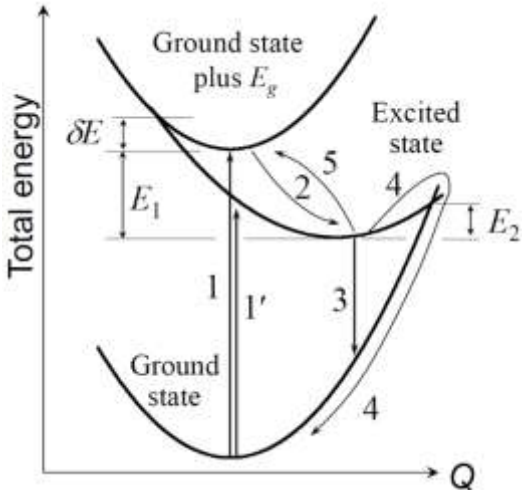

Figure 1. One-dimensional configuration coordinate diagram for an acceptor with the –/0 transition level at E_1 above the valence band in an *n*-type semiconductor. The ground and excited states correspond to the negatively charged and neutral acceptor, respectively. Transition 1 corresponds to above-bandgap excitation. Transition 1′ is a resonant excitation of an electron from the acceptor level to the conduction band. Transition 2 is a capture of a hole from the valence band by the acceptor, in general over the barrier δE. Transition 3 is a recombination of a free electron with the bound hole, resulting in PL. Transition 4 is a nonradiative recombination of a free electron and bound hole over the barrier E_2. Transition 5 is a thermal emission of the bound hole to the valence band.

An alternative explanation is that the slope of PL quenching reveals the ionization energy of an acceptor or a donor participating in the PL (Schön-Klasens mechanism).[7,8] In this case, bound holes are thermally emitted to the valence band (transition 5 in Figure 1) or bound electrons are thermally emitted to the conduction band. This mechanism requires the presence of other recombination channels (multicenter mechanism), including nonradiative centers through which the thermally emitted holes or electrons recombine. In this mechanism, the activation energy in Equation (1) is equal to the ionization energy (E_1 or $E_1 + \delta E$). The parameter C is proportional to the PL lifetime and the effective hole-capture coefficient.

A third mechanism has been suggested recently: the abrupt and tunable quenching of PL, in which defect-related PL intensity suddenly drops at some critical temperature.[9] The apparent

"activation energy" of the quenching (the slope in the Arrhenius plot) has no physical meaning in this case, and the critical temperature can be tuned over wide range by the excitation intensity. This exotic behavior is caused by a population inversion at low temperatures and a sudden redirection of the recombination flow from radiative to nonradiative defects upon achieving a critical temperature. We find that this mechanism of PL quenching is common for high-resistivity semiconductors.

In this paper, most important cases of PL quenching are reviewed. GaN is chosen as the case study. Deep understanding of PL from defects in GaN became possible due to advances in growth of high-quality GaN, optimal bandgap (E_g = 3.50 eV) for experimental and theoretical studies, high intensity of PL, and accumulated knowledge about defects in this material and their effects on PL.[10,11] Section 2 presents classic cases of PL quenching in GaN. Special cases, that are also critical, are reviewed in Section 3. In particular, a phenomenon sometimes called the "negative thermal quenching of PL" (a rise of PL intensity with increasing temperature) is explained. An increase or decrease of PL intensity with increasing temperature may be unrelated to thermal quenching, but rather be caused by a variation of the defect capture parameters or by specific experimental conditions or samples. Several interesting examples of PL quenching in other semiconductors are reviewed in Section 4. Some iconic cases are revisited with the aim to suggest alternative explanations to previously accepted models. Most of the examples in this work are for direct-bandgap semiconductors. PL from excitons and internal transitions in transition metals and rare earths are beyond the scope of this paper.

2. Mechanisms of Thermal Quenching of Photoluminescence in GaN

PL from defects in GaN is commonly quenched by the Schön-Klasens mechanism. Table I provides up-to-date information on defect-related PL bands commonly observed in GaN doped with major impurities or unintentionally doped.

Table I. Classification of defect-related PL bands in *n*-type or semi-insulating GaN

PL band	Attribution (transition level)	$\hbar\omega_{max}$ [a] [eV]	ZPL [eV]	E_A [b] [eV]	τ_0 [c] [μs]	C_p [cm^3/s]	C_n [cm^3/s]	Comments
RL1	? (–/0)	1.73	–	~1.2	220	3×10^{-7}	4×10^{-14}	*n*-type HVPE
RL2	? (donor)	~1.7	–	?	[10^2]			Insulating, Ga-rich, MBE, HVPE
YL1	C_N (–/0)	2.17	2.59	0.916	90	4×10^{-7}	1×10^{-13}	undoped, C-, Si-doped, HVPE, MOCVD, MBE
BL_C	C_N (0/+)	2.85	–	~0.3	[10^{-3}]	$\sim10^{-10}$		HVPE, MOCVD, "secondary" band
GL1	? (0/+)	2.35	–	~0.5	[2]	$\sim10^{-7}$		HVPE, "secondary" band
GL2	V_N (+/2+)	2.33	–	~0.43	[250]			Insulating, Ga-rich, MBE, MOCVD, HVPE
BL1	Zn_{Ga} (–/0)	2.86	3.10	0.40	15	5×10^{-7}	7×10^{-13}	Undoped, Zn-doped, MOCVD, HVPE
BL2	C_NH_i (0/+)	2.96	3.33	0.15	[0.3]			Insulating, MOCVD, HVPE
UVL	Mg_{Ga} (–/0)	3.28	3.28	0.223	3	1×10^{-6}	3×10^{-12}	Undoped, Mg-doped, all growth methods

a) The spectra are multiplied by λ^3 to present the number of emitted photons as a function of photon energy.
b) Position of defect level above the valence band maximum.
c) For eA transitions when $n = 10^{17}$ cm^{-3}. The values in square brackets are for internal transitions at $T < 20$ K.

Although it was proposed earlier that the GL2 and RL2 bands are quenched by the Seitz-Mott mechanism,[11] an alternative explanation will be given in Section 2.3. A new mechanism of thermal quenching is proposed for semi-insulating materials. Below, the classic cases of PL quenching in GaN are reviewed, while special cases will be analyzed in Section 3.

2.1. Conducive *n*-Type

In conductive *n*-type GaN (undoped or lightly doped with Si, Ge, or O), the Fermi level is located close to the conduction band, and defect-related PL bands at low temperatures ($T < 30$ K) are caused by electron transitions from shallow donors to various acceptors, the so-called donor-acceptor pair (DAP) recombination.[11,12] At low excitation intensity, all acceptors and deep donors remain almost completely filled with electrons. Then, the relative PL intensity or the absolute internal quantum efficiency of PL via a particular type of defect, η_i, (in general, the recombination efficiency via the i^{th} channel) depends only on the concentration of defects, N_i, and their hole-capture coefficient, C_{pi},[11]

$$\eta_i = \frac{I_i^{PL}}{G} = \frac{C_{pi} N_i}{\sum_j^m C_{pj} N_j}, \qquad (2)$$

where G is the electron-hole generation rate in unit volume from which PL originates, and m is the number of recombination channels, which include nonradiative and band-to-band recombination. Negatively charged acceptors capture holes much more efficiently than neutral donors. As a result, in undoped GaN with trace amounts of C, Zn, and Mg impurities, strong PL bands related to DAP transitions involving the C_N, Zn_{Ga}, and Mg_{Ga} acceptors are observed. These are the yellow luminescence (YL1) band with a maximum at 2.2 eV, the blue luminescence (BL1) band with a maximum at 2.9 eV, and the UV luminescence (UVL) band with a maximum at 2.26 eV, respectively (Table I). In undoped GaN samples grown by hydride vapor phase epitaxy (HVPE), the red luminescence (RL1) band with a maximum at 1.7-1.8 eV is also often observed and attributed to transitions from shallow donors to an unknown acceptor with the charge transition level at about 1.2 eV above the valence band. In time-resolved PL experiments, nonexponential decay of PL is observed for all these PL bands, in agreement with the theory of DAP transitions.[12]

With increasing temperature, electrons at shallow donors are thermally emitted to the conduction band, and at $T > 50$ K transitions from the conduction band to various acceptors (eA transitions) replace the DAP transitions. Since the nonradiative capture of holes by acceptors is much faster than eA or DAP recombination, the replacement of the DAP mechanism with the eA one is not expected to cause any change in PL intensity (or in η_i).[11] Note that, according to Equation (2), η_i varies with temperature if C_{pi} has temperature dependence, or if efficiency of any other recombination channel (strong enough to affect the behavior of the denominator in the equation) changes with temperature. In degenerate *n*-type GaN, eA transitions are dominant at any temperature, and the $I^{PL}(T)$ dependence is very similar to that in nondegenerate GaN.

Figure 2 shows examples of $I^{PL}(T)$ dependences for the YL1 and UVL bands in GaN. At low temperatures PL intensity is constant, and above a critical temperature T_0, it decreases exponentially, in agreement with Equation (1). The parameter E_A found from the fit (see the

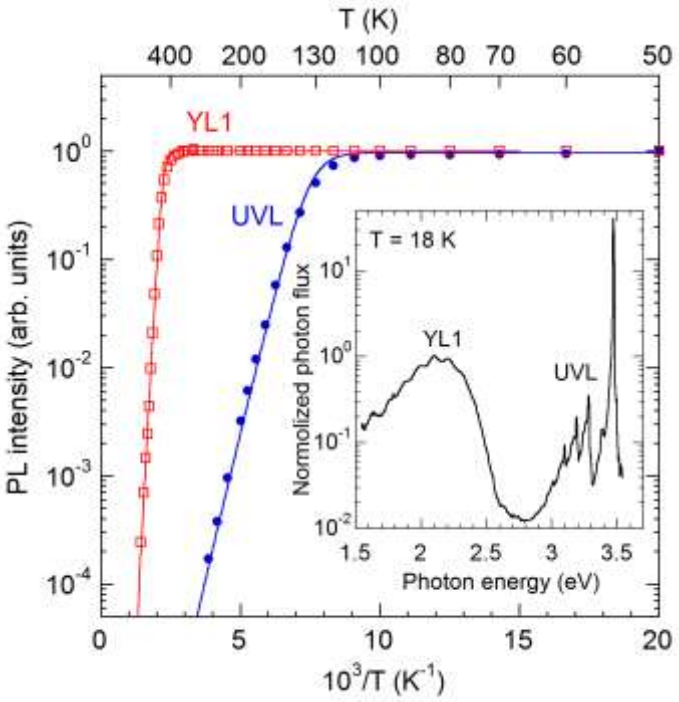

Figure 2. Normalized temperature dependences of the YL1 intensity in undoped, *n*-type GaN (sample svt750 grown by MBE) and the UVL intensity in Mg-doped *n*-type GaN (sample 3590 grown by HVPE). The lines are calculated using Equations (1) and (3) with the following parameters: E_A = 835 meV, η_{i0} = 0.1, τ_{i0} = 5×10^{-4} s, C_{pi} = 3×10^{-7} cm^3/s for the YL1 band and E_A = 186 meV, η_{i0} = 0.8, τ_{i0} = 17 μs, C_{pi} = 1×10^{-6} cm^3/s for the UVL band. The values of τ_{i0} were found from time-resolved PL experiments. The inset shows the PL spectrum for sample svt750 at T = 18 K.

caption) is very close to the value of the –/0 transition level for these acceptors at T < 50 K: 916±3 meV for the C_N responsible for the YL1 band and 223±2 meV for the Mg_{Ga} responsible for the UVL band.[13] Note that the ionization energy of acceptors may decrease with increasing temperature, along with the decrease in the bandgap. In this fit, the Schön-Klasens mechanism of thermal quenching is assumed, and the expression for the parameter C is obtained from solution of a system of rate equations:[9,14]

$$C = (1-\eta_{i0})\tau_{i0} C_{pi} N_V g^{-1}, \qquad (3)$$

where τ_{i0} and η_{i0} are the PL lifetime and the absolute internal quantum efficiency of PL via i^{th} type of defect at temperatures below the quenching, N_V is the effective density of states in the valence band, and g is degeneracy of the defect level. The value of η_{i0} can be estimated from comparison of integrated PL intensities at low temperatures with those in calibrated samples. The PL lifetime can be directly measured in time-resolved PL experiments, where nearly exponential decay of PL after a laser pulse is observed for defect-related bands, including UVL, BL1, YL1, and RL1 bands in *n*-type GaN at T > 50 K.[15] Assuming g = 2 and m_h^* = 0.8m_0, we have found from analysis of a large set of GaN samples that C_{pi} is about 1×10^{-6}, 5×10^{-7}, 4×10^{-7}, and 3×10^{-7} cm^3/s for acceptors responsible for the UVL, BL1, YL1 and RL1 bands, respectively, and the capture coefficients are nearly independent of temperature.

2.2. Conductive *p*-Type

It may be expected that transitions in *p*-type GaN mirror those in *n*-type, because the competition for electrons as minority carriers should govern the PL intensities. This is not exactly the case, at least for GaN, because the shallowest acceptor (Mg_{Ga} in GaN) is relatively deep, and the concentration of free holes is too low at $T < 200$ K. Then, in *p*-type GaN, where the Fermi level is near the Mg_{Ga} level (about 0.2 eV above the valence band), PL due to electron transitions from shallow or deep donors to the valence band is not observed, because the concentration of free holes is very low. In *p*-type GaN:Mg samples grown by molecular beam epitaxy (MBE), the UVL band (also labeled UVL_{Mg}) is the dominant PL band.[16] The UVL_{Mg} band is commonly composed of unresolved eA- and DAP-type transitions involving shallow donors and Mg_{Ga} acceptors. The PL decay after a laser pulse is fast (the apparent PL lifetime is shorter than 10 ns) due to fast escape of photogenerated electrons from the conduction band via unknown deep-level nonradiative centers.[17] This competition for electrons explains why the UVL_{Mg} intensity in *p*-type GaN:Mg is typically low.

With increasing temperature, the UVL_{Mg} intensity decreases with an activation energy corresponding to the ionization energy of shallow donors (**Figure 3**). This behavior is explained

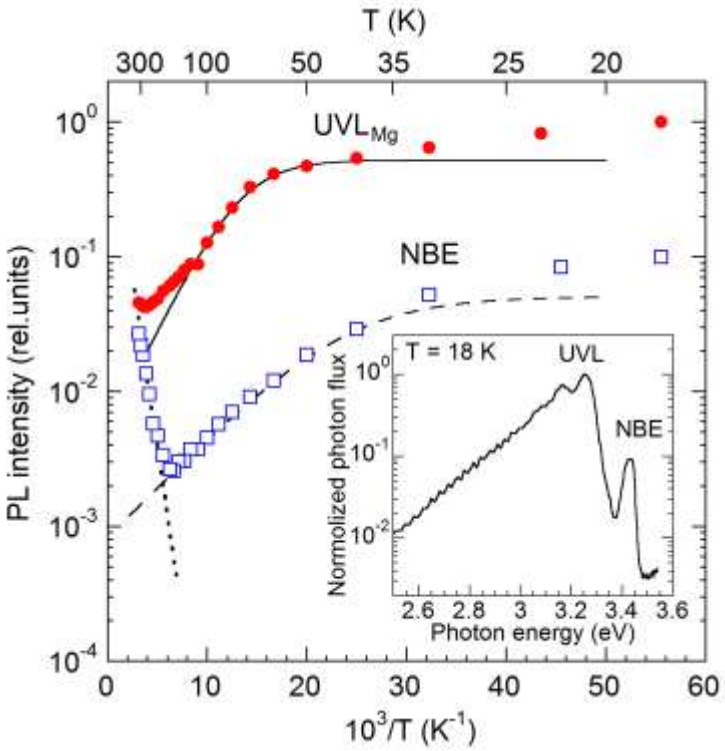

Figure 3. Temperature dependence of the peak UVL_{Mg} and NBE intensities in Mg-doped GaN (sample 9600A grown by MBE). The solid and dashed lines are calculated using Equation (1) with the following parameters: $I^{PL}(0) = 0.52$, $E_A = 30$ meV, and $C = 100$ for the UVL band and $I^{PL}(0) = 0.05$, $E_A = 15$ meV, and $C = 60$ for the NBE band. The dotted line shows the calculated dependence $1.3\times\exp(-\Delta E/kT)$ with $\Delta E = 0.1$ eV. The inset shows the PL spectrum at $T = 18$ K.

by the Schön-Klasens mechanism and caused by thermal emission of photogenerated electrons from shallow donors to the conduction band and their re-capture by nonradiative defects. Interestingly, the near-band-edge (NBE) emission intensity rises with temperature, while the quenching of the UVL_{Mg} band slows down with increasing temperature at $T > 200$ K (Figure 3). The NBE intensity is equal to Bnp, where n and p are the concentrations of free electrons and holes, respectively, and B is the radiative recombination coefficient. For GaN, $B \approx 2\times10^{-11}$ cm^3/s at room temperature, and it increases with decreasing temperature.[18,19,20] The $B(T)$ dependence may explain the decrease in the NBE intensity between 30 and 150 K. However, the exponential increase in the NBE intensity at $T > 200$ K can only be attributed to the increase in p with $E_A \approx$ 0.15 eV, because n remains nearly independent of temperature. Such behavior of the UVL_{Mg} and

NBE intensities is a hallmark of *p*-type conductivity.[17] It is possible that transitions from shallow donors to the valence band also contribute to the NBE band, remaining unresolved.

In *p*-type GaN:Mg grown by metalorganic chemical vapor deposition (MOCVD), the blue luminescence (BL_{Mg}) band with a maximum at about 2.8 eV is the dominant PL band. It is caused by DAP-type transitions involving a deep donor (with the level at about 0.5 eV below the conduction band) and the shallow Mg_{Ga} acceptor.[21,22,23,24] Slow, nonexponential decay of the BL_{Mg} intensity after a laser pulse agrees with the DAP model of the PL band.[25,26] The identity of the donor is not established, yet it is known that it is formed due to self-compensation effect, and the wave function for the bound electron is localized. Unlike *n*-type, where the wave function of electrons at shallow donors is diffuse and DAP transitions are observed for pairs with large separations, pairs with small separations are responsible for the BL_{Mg} band in *p*-type GaN. Strong Coulomb interaction in these pairs explains a significant shift of the BL_{Mg} band with variation of excitation intensity (by up to 0.2 eV).[17,23] With increasing temperature, the BL_{Mg} intensity decreases above 150-250 K with the activation energy of about 0.25-0.5 eV.[23,27] This quenching of PL is caused by thermal emission of electrons from the deep donors to the conduction band and the following recombination via other channels (Schön-Klasens mechanism).

2.3. Semi-insulating GaN

GaN samples are considered to be high-resistivity or semi-insulating when the concentration of free electrons or holes at room temperature is below the sensitivity limit of electrical measurement methods. Examples are Fe-, Zn- or C-doped GaN, where the concentration of acceptors exceeds the concentration of shallow donors and the Fermi level is located close to the

–/0 transition level of the Fe_{Ga} (0.6-0.7 eV below the conduction band),[28,29] Zn_{Ga} (0.35-0.40 eV above the valence band),[9] or C_N (~0.9 eV above the valence band).[30,31] Note that the concentrations of donors and acceptors do not need to be close to each other (high compensation ratio) to make a wide-bandgap semiconductor semi-insulating.

For high-resistivity semiconductors, a third mechanism of PL quenching has been recently suggested: the abrupt and tunable quenching.[9] The temperature dependence of a defect-related PL can be formally described with Equation (1); however the parameters not always have a physical meaning. An example is shown in **Figure 4** for the YL1 band in C-doped GaN.

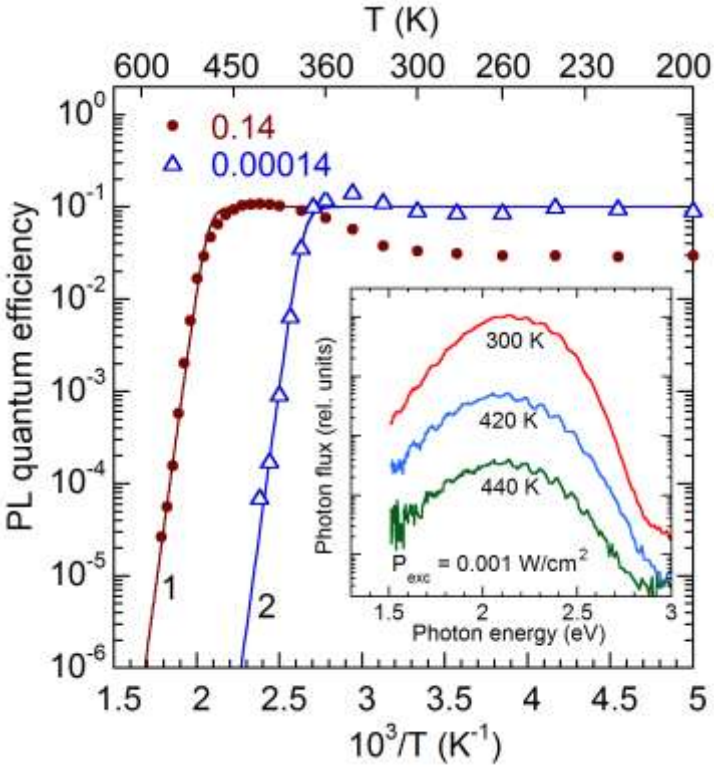

Figure 4. Temperature dependence of the YL1 quantum efficiency in C-doped GaN (sample cvd4229 grown by MOCVD) at P_{exc} = 0.00014 and 0.14 W/cm^2. The lines are calculated using Equation (1) with the following parameters: C = 1.2×10^{27} (1) and 5×10^{34} (2), and E_A = 2.6 eV (both 1 and 2). The rise of PL intensity with increasing temperature from 300 to 400 K is explained in Section 3.2.3.The inset shows the evolution of PL spectrum with increasing temperature from 300 to 440 K at P_{exc} = 0.001 W/cm^2.

In conductive *n*-type GaN samples, the quenching of the YL1 band begins at $T_0 \approx 450$ K (Figure 2), and the activation energy in the quenching region is 0.8-0.9 eV, very close to the ionization energy of the C_N acceptor (0.916 eV at $T < 50$ K). Note that T_0 is independent of the excitation intensity in these samples (at least at low excitation intensity). In high-resistivity samples, the apparent "activation energy" my reach 2.6 eV and T_0 increases with excitation intensity, i.e., the quenching is abrupt and tunable by excitation intensity (Figure 4). While similar PL behavior and related superlinear increase of PL intensity in the region of PL quenching were reported for other semiconductor systems in the past,[32,33] only recently an explanation has been found.[9] The model that explains all the features of this unusual quenching behavior should include at least three types of defects: a shallow donor *D*, a radiative defect (acceptor *A*) and a nonradiative defect (e.g., a deep donor *S*) with concentrations N_D, N_A, and N_S, respectively, and capture coefficients C_{pi} and C_{ni} where $i = D, A, S$. At low temperatures, a population inversion occurs in the gap in conditions of steady-state PL due to fast capture of photogenerated holes by acceptors *A* and fast capture of photogenerated electrons by deep donors *S*. Slow radiative transitions of electrons from shallow donors (DAP) or from the conduction band (eA) to the acceptors produce PL with high efficiency, because the nonradiative channel is saturated and blocked by electrons accumulated at *S* centers. This blockade may also result in accumulation of electrons in the conduction band and a conversion of the conductivity type from *p* to *n*.[9,34]

The abrupt quenching of the PL occurs at a critical temperature T_0, when the concentration of holes in the valence band, which are thermally emitted from the acceptor, p_{therm}, becomes equal to the concentration of optically generated holes, p_{opt}. The T_0 increases with

increasing excitation intensity (P_{exc} or G) because $p_{opt} \propto G$ and $p_{therm} \propto \exp(-E_A/kT)$. The following formula has been derived for this case: [9]

$$T_0 = \frac{E_A}{k \ln(B/G)} \quad (4)$$

with

$$B = C_{pA}\left(\frac{1}{\eta_{A0}} - 1\right)(N_A - N_D)\frac{N_V}{g}. \quad (5)$$

The drop of PL intensity near T_0 may be very abrupt (nearly vertical in the Arrhenius plot), so that the "activation energy" or the measured slope has no physical meaning. However, the ionization energy E_A can be found from the fit of the $T_0(G)$ dependence by using Equation (4). Indeed, the dependence of $1/T_0$ on $\ln(G)$ is a straight line of the form $y = a - bx$ with $b = k/E_A$.[35]

The abrupt and tunable quenching was first observed and explained for the BL1 band in Zn-doped GaN.[9] In agreement with the model, other PL bands, including excitonic emission, abruptly drop at T_0. The dominant nonradiative defect remains unknown, yet it is expected to be a deep donor with parameters satisfying the following inequality: $(C_{pS}C_{nD})/(C_{nS}C_{pA}) << 1$. Later, this type of quenching was found for PL in Mg-doped GaN,[17,36] C- and Fe-doped GaN,[37] Be-doped GaN,[38] and Li-doped ZnO.[39] More complicated case, the two-step tunable quenching in Zn-doped GaN (**Figure 5**) was explained with a similar model, which included an additional acceptor.[40] In all these examples, samples are semi-insulating.

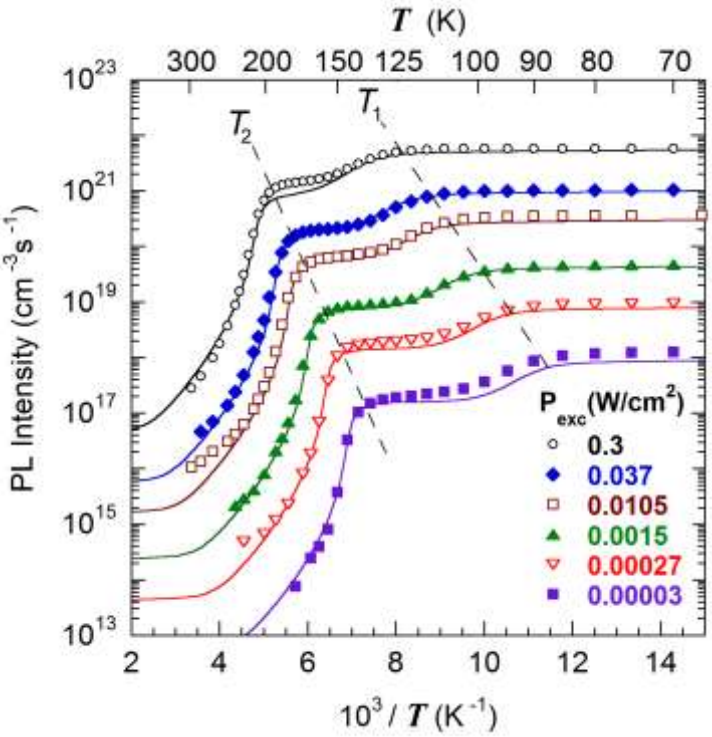

Figure 5. Temperature dependence of PL intensity for the BL1 band in GaN:Zn (sample s560 grown by HVPE) at selected excitation intensities. The solid curves are from numerical solution of rate equations for a model involving four types of defects. The dashed lines show schematically the shift of the characteristic temperatures of PL quenching with variation of excitation intensity. Reprinted with permission from [M. A. Reshchikov, "Two-step thermal quenching of photoluminescence in Zn-doped GaN", Phys. Rev. B **85**, 245203 (2012)], Copyright © 2012 by the American Physical Society.

In semi-insulating, undoped GaN, PL bands caused by internal transitions (from an excited state to the ground state, both located in the gap) are sometimes observed.[41] These are the BL2 band with a maximum at 3.0 eV and ZPL at 3.33 eV, assigned to the C_NH_i complexes, the GL2 band with a maximum at 2.3 eV, assigned to the nitrogen vacancy (V_N), and the RL2 band with a maximum at 1.7-1.8 eV from unknown defect (Table I). All three defects are presumably deep donors with excited states located close to the conduction band. Transitions from the excited state to the ground state cause exponential decay of PL in time-resolved PL measurements even at $T \approx 15$ K. The quenching of the BL2 band in steady-state PL with E_A = 0.15 eV is explained by thermal emission of holes from the 0/+ level of the C_NH_i defect to the

valence band.[30,42] The GL2 and RL2 bands are quenched with $E_A \approx 0.1$ eV with increasing T from 100 to 200 K.[11] This small activation energy contrasts with deep optical energies for these two bands, and the quenching was initially explained with the Seitz-Mott mechanism with $E_A = E_2$ in Figure 1.[11] Later, it was found that at $T > 200$ K the GL2 band is quenched with a larger activation energy ($E_A \approx 0.4$ eV).[43] A model has been suggested for the V_N defect, according to which the two activation energies were attributed to thermal emission of electrons from the excited state to the conduction band (0.1 eV) and holes from the ground state to the valence band (0.4 eV). Less is known about the defect responsible for the RL2 band, yet its quenching with $E_A \approx 0.1$ eV can also be explained by thermal emission of electrons from an excited state to the conduction band. Thus, the Seitz-Mott mechanism seems unlikely for the RL2 and GL2 bands in GaN.

3. Peculiarities of Thermal Quenching of Photoluminescence in GaN

3.1. Variations in Quenching Behavior

3.1.1. Critical Temperature of Quenching

According to Equations (1) and (3), the critical temperature T_0 for PL in conductive *n*-type GaN shifts to higher temperatures with decreasing τ_{i0}. For electron transitions from the conduction band to acceptors in *n*-type GaN, the decay of PL intensity after a laser pulse is nearly exponential, and the characteristic time of this decay, the PL lifetime τ_{i0}, is inversely proportional to the concentration of free electrons n: [15,44]

$$\tau_{i0} = \frac{1}{C_{ni} n}. \qquad (6)$$

Here, C_{ni} is the electron-capture coefficient, which is about 3×10^{-12}, 7×10^{-13}, 1×10^{-13}, and 4×10^{-14} cm^3/s for acceptors responsible for the UVL, BL1, YL1 and RL1 bands, respectively.[15] Thus, for samples with different concentrations of free electrons the quenching is observed at different temperatures.

An example for the Zn_{Ga}-related BL1 band in *n*-type GaN is shown in **Figure 6**. In undoped GaN (with $n = 10^{16}$–10^{17} cm^{-3}), the BL1 band is quenched at $T > 200$ K with $E_A \approx 0.35$ eV (samples 1611 and 2015). However, in Si-doped GaN (sample 1142), where PL lifetime for all defect-related PL bands is shorter, T_0 is higher. An exceptionally high η_{i0} for the BL1 band in sample 1142 results in additional shift in T_0, so that the PL quenching begins only at $T_0 \approx 270$ K.

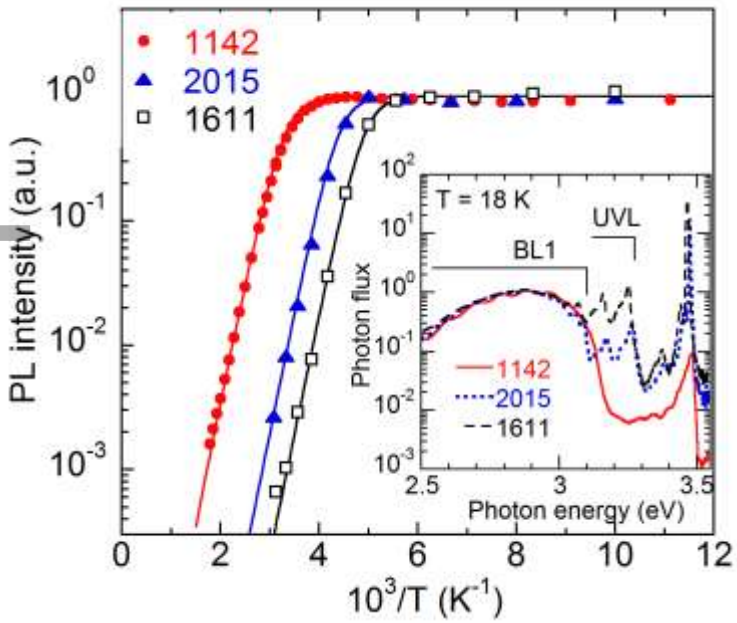

Figure 6. Temperature dependence of the BL1 intensity (normalized at low temperature) in undoped GaN (samples 2015 and 1611 grown by HVPE) and GaN co-doped with Si and Zn (sample 1142 grown by MOCVD), at $P_{exc} \approx 0.0001$ W/cm^2. The lines are calculated using Equations (1) and (3) with the following parameters: $E_A = 330$ meV, $\eta_{i0} = 0.85$, $\tau_{i0} = 5\times10^{-7}$ s for sample 1142; $E_A = 335$ meV, $\eta_{i0} = 0.1$, $\tau_{i0} = 1.5\times10^{-5}$ s for sample 2015; $E_A = 340$ meV, $\eta_{i0} = 0.07$, $\tau_{i0} = 1.3\times10^{-4}$ s for sample 1611; C_{pi} =

5×10^{-7} cm^3/s for all the samples. The values of τ_{i0} were found from time-resolved PL experiments. The inset shows PL spectra at T = 18 K.

Examples of strong dependence of T_0 on n for the YL1 band in undoped and Si-doped GaN samples can be found in Ref. [37]. While in undoped GaN the quenching of the YL1 band normally begins at ~450 K, it may begin at much higher temperatures in degenerate, Si-doped GaN. The smoothening of the quenching dependence and large shift of T_0 in heavily doped samples can make a false impression of abnormally low E_A due to limited range of accessible temperatures.[37] It is also important to study temperature dependence of PL at low excitation intensities to avoid saturation of defects with photogenerated charge carriers. The latter may cause an artificial shift of T_0 to higher temperatures and a distortion of the $I^{PL}(T)$ dependence, as will be demonstrated in Section 3.3.2.

3.1.2. Temperature Dependence of Luminescence Lifetime

With increasing temperature in conductive, *n*-type GaN, the PL lifetime *measured* in time-resolved PL experiments changes very similar to the PL intensity and can be fitted with the following expression:[15,44]

$$\tau_i(T) = \frac{\tau_{i0}}{1 + C\exp\left(-\frac{E_A}{kT}\right)}, \qquad (7)$$

where C and τ_{i0} are given by Equations (3) and (6), respectively. The only difference with the dependence given by Equation (1) is that τ_{i0} slowly decreases with temperature in nondegenerate samples, which reflects increasing n due to thermal emission of electrons from shallow donors to the conduction band, whereas τ_{i0} is independent of temperature in degenerate GaN.[15] From analysis of the $I^{PL}(T)$, $\tau_{i0}(T)$, and $n(T)$ dependences, we can also determine if there is any temperature dependence of the C_{ni} and C_{pi}.

Examples for the BL1 band are shown in **Figure 7**. The concentration of free electrons in undoped GaN (sample 1611) is about 2×10^{16} cm^{-3} at room temperature, and τ_{i0} decreases with increasing T from 100 to 200 K in agreement with the $n(T)$ dependence and Equation (6).[15] In Si-doped GaN (TD1140), $n \approx 10^{18}$ cm^{-3} at T = 100-300 K, and the τ_{i0} dependence can be ignored. Note that the PL intensity remains independent of temperature up to 170 K in both cases. These examples show that coefficients C_{nA} and C_{pA} for the Zn_{Ga} acceptor are independent of temperature. The difference between the $I^{PL}(T)$ and $\tau_{i0}(T)$ dependences at T > 180 K for sample TD1140 will be explained in Section 3.2.2. More examples, that reveal no temperature dependence of the C_{nA} and C_{pA} for the dominant PL bands in undoped GaN can be found elsewhere.[15]

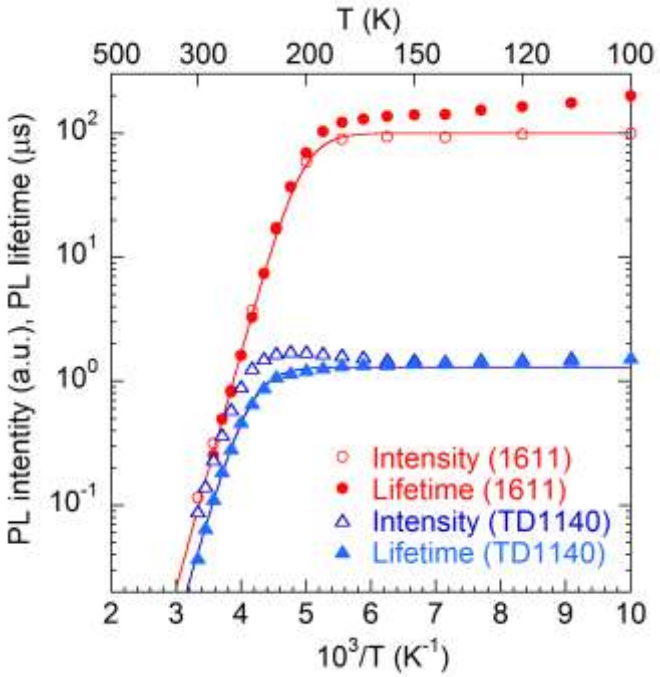

Figure 7. Temperature dependence of PL intensity and PL lifetime for the BL1 band in Si-doped GaN (sample TD1140 grown by HVPE) and undoped GaN (sample 1611 grown by HVPE). The PL intensity dependences are shifted arbitrarily in vertical direction to match the lifetime dependences. The lines are calculated using Equations

(1) and (3) with the following parameters: E_A = 340 meV, τ_{i0} = 140 μs for sample 1611; E_A = 320 meV and τ_{i0} = 1.5 μs for sample TD1140; C_{pi} = 5×10^{-7} cm^3/s for both samples.

It should be kept in mind that the $\tau(T)$ dependence is not always similar to the $I^{PL}(T)$ dependence, and sometimes it cannot be described with Equation (7). An example is the GL1 band, identified as a secondary PL band (i.e., observed only after a defect captures two holes) of unknown defect in GaN grown by HVPE. The defect is most likely not related to carbon,[30] in contrast to what was initially proposed.[45,46] The $I^{PL}(T)$ dependence for the GL1 band can be fitted with Equations (1) and (3) in a wide range of temperatures (**Figure 8**). However, τ_{i0} increases between 80 and 280 K as $\tau_{i0} = \tau_1 + \tau_2$, where $\tau_1 = aT^3$ with a = 2×10^{-12} s/K^3, and τ_2 = 1.5 μs. The unusual increase of τ_{i0} with temperature was explained in a model where the GL1 band is caused by internal transitions from an excited state located close to the conduction band to the ground 0/+ state located at about 0.5 eV above the valence band.[46] The excited state behaves as a classic giant

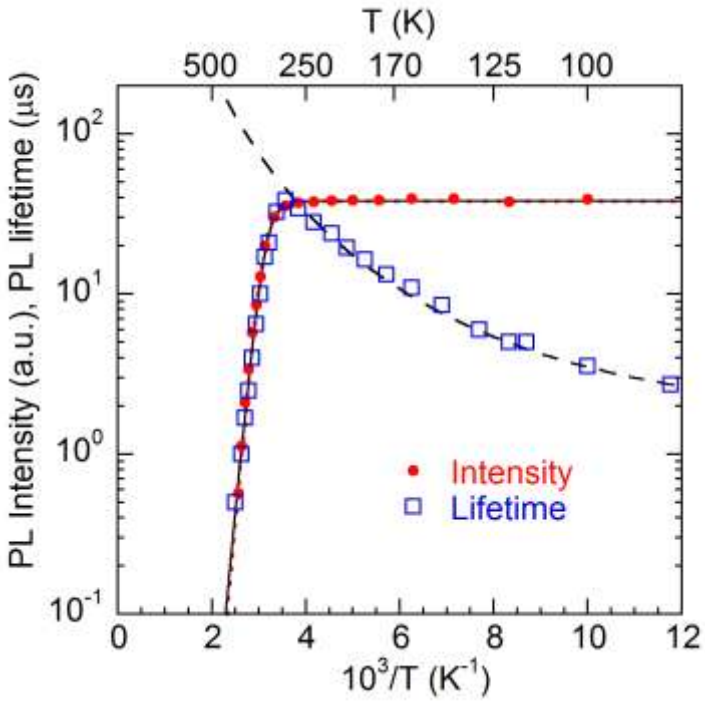

Figure 8. Temperature dependence of PL intensity and PL lifetime for the GL1 band in undoped bulk GaN (sample B73 grown by HVPE). The PL intensity curve is shifted arbitrarily in vertical direction to match the lifetime dependence in the region of PL quenching. The solid line is calculated using Equations (1) and (3) with the following parameters: η_{i0} = 0.1; E_A = 550 meV; C_{pi} = 1.6×10^{-6} cm^3/s; and τ_{i0} = 40 μs. The dashed line is the dependence $\tau_{i0}(T)$ = [2(T/100)^3+1.5] μs according to the model of the optically-generated giant trap.[46] The dotted curve for the $I^{PL}(T)$ dependence (undistinguishable from the solid curve) is calculated with the following parameters: η_{i0} = 0.1, E_A = 490 meV, C_{pi} = 1×10^{-7} cm^3/s, and the $\tau_{i0}(T)$ dependence given above.

trap,[47] and the temperature-dependent component τ_1 describes the capture of free electrons by this state. The τ_2 is the characteristic time of the internal transition. In time-resolved PL experiments, the slower of the components governs the measured characteristic time of the GL1 intensity decay after a laser pulse.[46] At T > 300 K, both PL intensity and PL lifetime decrease exponentially, with E_A ≈ 0.5 eV (Figure 8), and the dependences can be fitted with Equations (1), (3), and (7). If one ignores the temperature dependence of τ_{i0} at T > 300 K, the parameters of the fit would be: E_A = 550 meV and C_{pi} = 1.6×10^{-6} cm^3/s. The obtained hole-capture coefficient appears to be too high for the capture by a neutral donor-like state. However, if we extrapolate the $\tau_{i0}(T)$ dependence as shown with a dashed line in Figure 8, a nearly identical $I^{PL}(T)$ dependence can be obtained using Equations (1) and (3) with E_A = 490 meV and C_{pi} = 1×10^{-7} cm^3/s.

3.1.3. Temperature Dependence of the Hole-Capture Coefficient

In most of examples shown above, the PL intensity is independent of temperature at T < T_0, which indicates that the C_{pi} is temperature-independent for the considered defects, see Equation (2). However, in general, the hole-capture coefficient for deep-level defects may significantly increase with temperature.[48,49] This increase can be better understood with the help of the configuration coordinate diagram (Figure 1). The capture of a free hole by an acceptor is

transition 2 in Figure 1. Depending on the shapes and relative positions of the adiabatic potentials, there may be a barrier δE or no barrier for such transition.

Let us consider the C_N acceptor, which is responsible for the YL1 band in GaN. First-principles calculations predict a barrier $\delta E \approx 0.49$ eV for the capture of holes by the C_N acceptor.[50] As a result, the C_{pi} is expected to increase by two orders of magnitude as the temperature increases from 20 to 600 K. This prediction contradicts the experimental data. Indeed, according to Equation (2), the PL intensity before its quenching is proportional to the C_{pi}, and no variation of PL intensity with temperature can be noticed for the YL1 band (Figure 2). Only in samples with very high quantum efficiency of excitonic emission, the YL1 and other defect-related PL intensities increase simultaneously with the quenching of the excitonic emission due to a competition of recombination channels as discussed in Section 3.2.1. It should be also kept in mind that the capture coefficient for attractive centers decreases with temperature as $T^{-1/2}$.[49] It is possible that a small barrier (much smaller than predicted $\delta E \approx 0.49$ eV) exists for the hole-capture by the C_N acceptor, but the related increase in the C_{pA} is compensated by the decrease due to attractive nature of the acceptor. Note that no significant $C_{pA}(T)$ dependence can be noticed also for other acceptors in unintentionally doped GaN (Mg_{Ga}, Zn_{Ga}, and unknown deep acceptor responsible for the UVL, BL1, and RL1 bands, respectively). This can be explained by favorable shapes and relative positions of the adiabatic potentials leading to small δE for these defects. On the other hand, it may be difficult to detect PL from defects with large δE, because the PL signal may be too weak.

3.1.4. Effect of the Surface on Luminescence Intensity

Slow decrease of PL intensity with increasing temperature can also be observed due to increasing band bending and depletion region width. Indeed, in conditions of steady-state PL, the band bending and depletion region width are small at low temperatures, and they increase with increasing temperature, because more and more electrons in *n*-type semiconductor (or holes in *p*-type) can reach the surface over the near-surface barrier and be trapped by surface states. In *n*-type GaN, the band bending in dark is about 1.0 eV, and the depletion region width depends on the concentration of uncompensated shallow donors. At moderate excitation intensities, the band bending decreases by 0.3-0.5 eV at room temperature.[51] PL intensity from the depletion region is low due to rapid separation of photogenerated electrons and holes by near-surface electric field. Thus, increasing with temperature band bending may result in a gradual decrease of PL intensity, especially in samples with wide depletion region.

3.2. "Negative" Thermal Quenching

PL intensity may increase with increasing temperature, a phenomenon sometimes called the "negative quenching". One example is a rise of the eA component of the Mg-related UVL emission.[11,17,40] At low temperature, transitions from shallow donors to the Mg_{Ga} acceptor are responsible for the UVL band with the strongest peak at about 3.26 eV. With increasing temperature, electrons are emitted from shallow donors to the conduction band, and a very similar PL band, shifted to higher energies by about 20 meV, emerges. Other typical examples are reviewed below.

3.2.1. Quenching of an Intense Luminescence Band

In samples with a very intense PL band, the quenching of this PL results in a rise of other PL bands. This is explained by a competition between recombination channels for photogenerated minority charge carriers. An example is shown in **Figure 9**. A PL spectrum from GaN co-doped

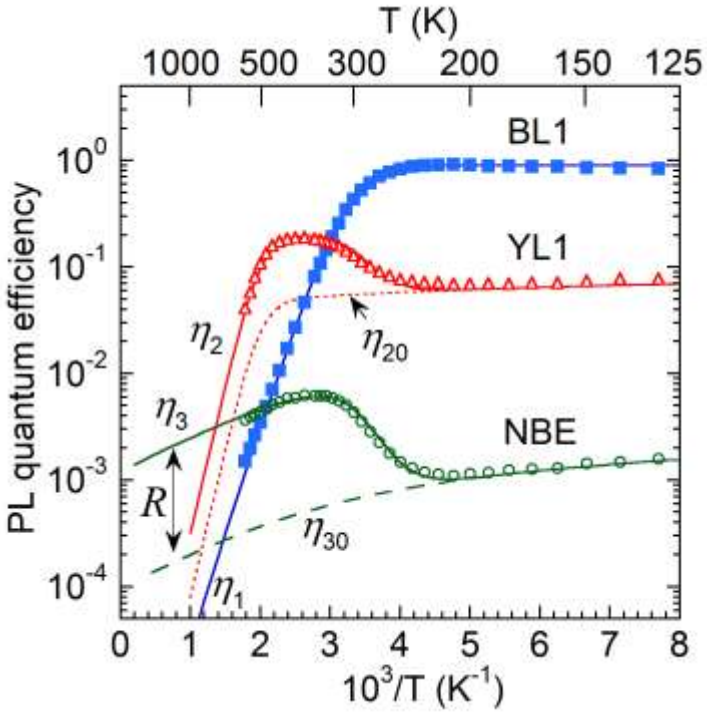

Figure 9. Temperature dependence of quantum efficiency for the BL1, YL1 and NBE bands in GaN:Si,Zn (sample 1142 grown by MOCVD). The lines are calculated. Parameters in $\eta_1(T)$ for the BL1 band are the same as in Figure 6. The $\eta_{20}(T)$ and $\eta_{30}(T)$ dependences are simulated to match low-temperature parts of the experimental dependences and the quenching of the YL1 band at $T > 500$ K with $E_A = 550$ meV. The $\eta_2(T)$ and $\eta_3(T)$ dependences are calculated using Equation (9) with $\eta_{10} = 0.75$ found from the $\eta_2(T)$ dependence and $\eta_{10} = 0.92$ from the $\eta_3(T)$ dependence.

with Si and Zn contains weak NBE and YL1 bands and a very strong BL1 band attributed to transitions from the conduction band to the Zn_{Ga} acceptor in degenerate *n*-type GaN.[52] The absolute internal quantum efficiency of the BL1 band at temperatures below its quenching was estimated by using independent methods, and for the sample analyzed in Figure 9 it is $\eta_{10} = 0.94$.

The quenching of the BL1 band is caused by thermal emission of holes from the Zn_{Ga} level to the valence band. These holes are re-captured by all recombination channels (the BL1, YL1 and NBE bands plus nonradiative recombination), so that the efficiency of each recombination channel, other than the BL1, increases by a factor of R:

$$R = \frac{1}{1 - \eta_{10}}. \quad (8)$$

If η_i are quantum efficiencies of the recombination channels benefiting from the quenching of the BL1 band (i = 2,3,4 for the YL1, NBE, and nonradiative recombination), and the expected temperature dependences not accounting for the quenching of the BL1 band, $\eta_{i0}(T)$, are known from analysis of other samples or from extrapolation of the low-temperature parts, then the $\eta_i(T)$ dependences can be can be found from the following expression:[52]

$$\eta_i(T) = \eta_{i0}(T)\frac{1 - \eta_1(T)}{1 - \eta_{10}}. \quad (9)$$

Observation of such behavior of PL is a solid proof of the Schön-Klasens mechanism for the BL1 quenching. Note that there may be other reasons for a rise of a defect-related PL band intensity with temperature (Sections 3.3.2 and 3.3.3). However, a rise of two or more PL bands simultaneously with the quenching of a very strong PL, and especially a rise of the NBE emission which is expected to fade with temperature in *n*-type GaN, should be considered as a strong argument for the above mechanism.

Another example is shown in **Figure 10**. The YL1 band in *n*-type GaN co-doped with Si and C has a very high quantum efficiency due to high concentration of C (7×10^{17} cm^{-3}) and large hole-capture coefficient ($C_{pA} \approx 4\times10^{-7}$ cm^3/s).[30] The quenching of the YL1 band is caused by thermal emission of holes from the C_N acceptors to the valence band. The NBE emission

intensity increases by a factor of 8, which indicates that the absolute internal quantum efficiency of the YL1 band at low temperatures is about 88%.

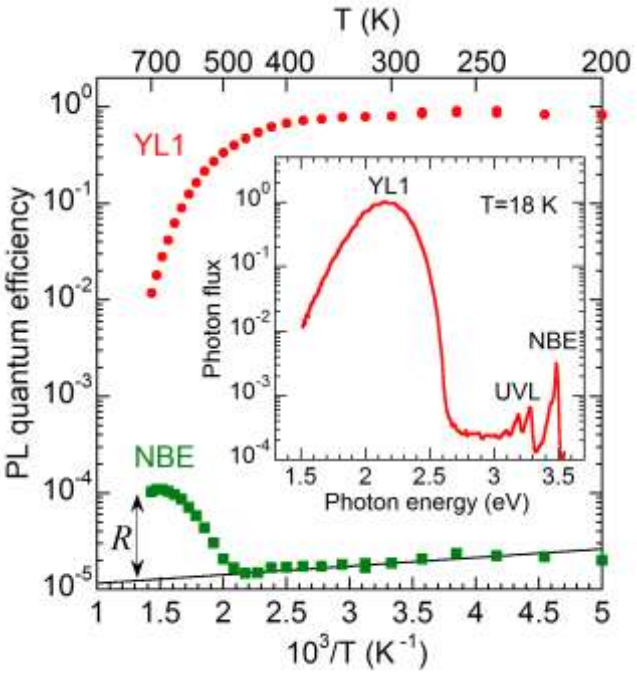

Figure 10. Temperature dependence of the quantum efficiency for the YL1 and NBE bands in GaN:Si,C (sample MD42 grown by MOCVD). The quenching of the YL1 band causes a rise of the NBE emission by a factor of R = 8, from which η_{10} = 0.88 can be calculated for the YL1 band from Equation (8). The inset shows low-temperature PL spectrum.

Other notable examples include the quenching of excitonic emission in ZnO,[53] and GaN,[14] and the UVL band in Mg-doped GaN.[17,53] If the quantum efficiency of a PL band is low before its quenching (e.g., η_{10} < 0.1), then the rise of other PL intensities may remain unnoticed. There are numerous examples of rising PL bands reported in the literature, yet not always the mechanism of the PL rise is recognized.

3.2.2. Quenching of a Nonradiative Channel

An interesting example is shown in **Figure 11**. Two PL bands (BL1 and NBE) rise (or at least

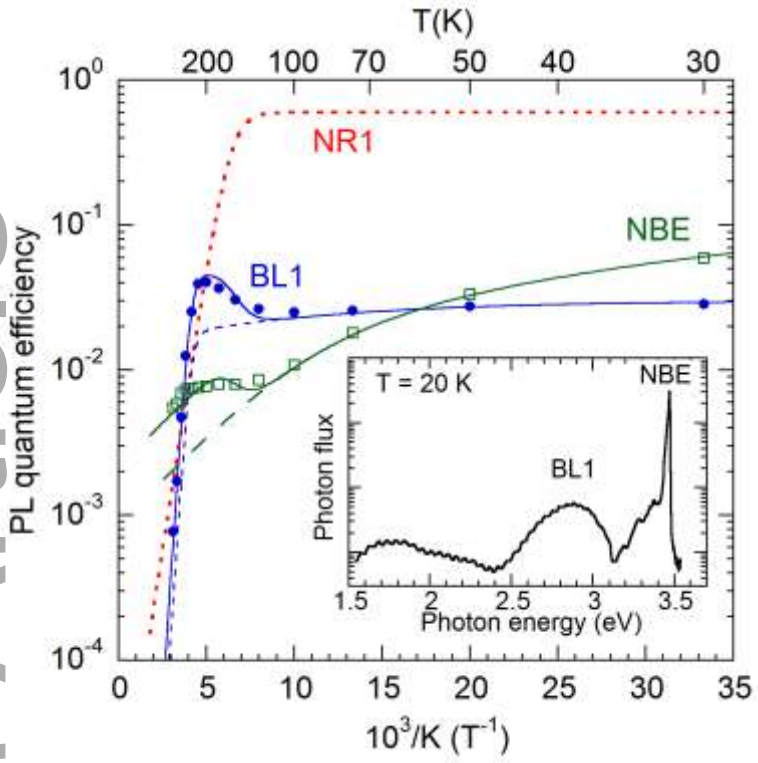

Figure 11. Temperature dependence of quantum efficiency for the BL1 and NBE bands in Si-doped GaN (sample TD1140 grown by HVPE). The quenching of the nonradiative channel NR1 causes a rise of the NBE and BL1 intensities by a factor of R = 2.5, from which η_{10} = 0.6 can be calculated for the NR1 with Equation (8). The dashed lines show expected temperature dependences of the BL1 and NBE efficiencies. The solid lines are calculated using Equation (9) with η_{10} = 0.6 for the nonradiative channel NR1. The dotted curve is predicted temperature dependence of the NR1 efficiency, the temperature dependence of which is described with Equation (1) with η_{10} = 0.6, C = 10^5, and E_A = 155 meV. The inset shows low-temperature PL spectrum.

deviate from their expected behavior) with increasing temperature from 130 to 200 K. However, there are no strong PL bands that are quenched at these temperatures. The temperature behavior of the PL bands in this sample can be explained if we assume that one of *nonradiative* recombination channels (NR1) is quenched at T > 130 K with the activation energy E_A = 155 meV. The efficiency of this channel is estimated to be 60% from the magnitude of the step in the BL1 and NBE (R = 2.5). The efficiencies of PL bands in this sample were estimated from comparison of integrated intensities with those in calibrated GaN samples.[9,54] Since the total quantum efficiency of all PL bands is below 10%, then at least 30% of the low-temperature

recombination efficiency should be attributed to another nonradiative source (NR2), which becomes the main recombination channel at $T > 200$ K. Remarkably, the rise of PL intensity with temperature in this sample does not cause a rise in τ_{i0} (Figure 7), in agreement with Equation (7).

3.2.3. Other Examples of Negative Thermal Quenching

The "negative thermal quenching" in semiconductors is widely observed and discussed in the literature. So Williams and Eyring [55] proposed that a rise of PL intensity by a factor of ~1.5 with increasing temperature from 225 to 280 K in ZnS:Ag is caused by a transition from a metastable excited to a stable excited state of a defect over a small barrier between these states. Yokogawa *et al.*[56] observed a rise of the 2.65-eV blue band in ZnO at temperatures between 180 and 300 K with an activation energy of ~0.1 eV and the quenching at higher temperatures with $E_A \approx 0.76$ eV. Similar behavior of PL was observed for PL in Zn-doped $CuAlS_2$,[57] Mg-doped GaN,[58] undoped ZnO,[59] ZnO nanostructures,[60] $BiFeO_3$ nanowires,[61] and other materials. Shibata [62] suggested that the negative thermal quenching is caused by thermal excitation of electrons from states lying below the initial state of PL transitions. Note that in some cases both the excitonic and defect-related PL increased in the same temperature range,[60] similar to an example shown in Figure 11 in Section 3.2.2. In other cases, there is no information about temperature behavior of other PL bands in studied samples. Davis [63] examined several cases of PL increase with temperature in Si. A significant increase in PL intensity from the P centers (carbon-oxygen complexes) was observed with increasing temperature from 4 to 30 K. It was explained by a release of excitons from very shallow traps and their re-capture by the P center. An exponential increase of PL intensity from the Cu+S center was explained by thermal excitation from the lower lying excited state (from which the radiative transition is forbidden) to a higher lying state, the transition from which is allowed.[63]

A careful analysis may be required to determine the reason of unusual temperature behavior of PL. For example, the C_N-related YL1 band is well understood and its behavior can be reliably predicted. Normally, its intensity remains independent of temperature up to ~400 K. In some samples the YL1 intensity slowly decreases with increasing temperature at $T < T_0$, which can be attributed to increasing band bending (Section 3.1.4). In other samples, it increases in certain range of temperatures. This increase can be assigned to the quenching of a very strong PL band in this temperature range (Figure 9) or to the quenching of a nonradiative channel. In particular, the rise of the YL1 band between 300 and 400 K in Figure 4 should be attributed to the quenching of a nonradiative recombination channel, because the NBE intensity in this sample also increases by a factor of 3 in the same temperature range (not shown). Other reasons that cause slow change in PL intensity at temperatures below its quenching and different activation energies in the quenching region are reviewed below.

3.3. Deviations in the Activation Energy

In the literature, thermal quenching of PL is often used to find the ionization energy for a defect and to differentiate between defects with similar PL bands that cannot be resolved. For example, Armitage *et al.*[64] compared the quenching of the yellow luminescence band in undoped and C-doped GaN samples. This work is often cited as an experimental proof that more than one defect is responsible for the yellow luminescence band in GaN. Those authors have found from the slope of the PL quenching that E_A = 650±30 meV for the undoped sample and E_A = 1040±60 meV for the C-doped GaN sample and concluded that two different defects cause similar in shape and position yellow bands: the gallium vacancy (V_{Ga}) and a C-related defect, respectively. However, as has been demonstrated recently,[37] the apparent slope in the quenching of the YL1

band in GaN may vary over wide range, from 0.06 to 1.8 eV, and in all cases the C_N-related YL1 band can be recognized by its ZPL at 2.59 eV and other characteristic parameters. From analysis of a great number of undoped, C- or Si-doped GaN samples grown by different methods, we could not find any evidence for the existence of the 2.2-eV (yellow) band not caused by the C_N defect. Moreover, the V_{Ga}–related defects are likely to be either nonradiative or very inefficient hole traps in GaN, and therefore do not contribute to the experimentally observed yellow band.[30] An alternative explanation of the dependences obtained by Armitage *et al*.[64] is given below.

3.3.1. Effect of Excitation Intensity on Quenching Dependence

The experiments in Ref. [64] were conducted at very high excitation intensity (P_{exc} = 20 W/cm^2). With increasing excitation intensity, the C_N-related YL1 band in undoped GaN normally saturates at $P_{exc} > 10^{-4}$–10^{-3} W/cm^2 (see the inset to **Figure 12**). In a simple model (assuming that electron-hole pairs are uniformly generated in the near-surface region with the width α^{-1}), the critical generation rate at which the saturation begins is $G_{cr} = N_A(\eta_0 \tau_0)^{-1}$, which corresponds to P_{exc}^{cr} = 10^{-4}–0.5 W/cm^2 for the following typical parameters: $N_A = 2\times10^{15}$–10^{17} cm^{-3}, τ_0 = 0.1-1 ms (for $n \approx 10^{17}$ cm^{-3}), and η_0 = 0.01-0.1. As a result, T_0 increases with increasing P_{exc} above P_{exc}^{cr} (see the **Appendix**), because PL intensity is saturated only at $T < T_0$. At $T > T_0$, holes are emitted to the valence band and the saturation is lifted. An example is shown in Figure 12, where T_0 = 450 K for $P_{exc} = 10^{-4}$ W/cm^2 and T_0 = 500 K for P_{exc} = 0.25 W/cm^2. Interestingly, not only T_0 shifts but also the slope of the quenching dependence decreases with increasing P_{exc} (Figure 12). This

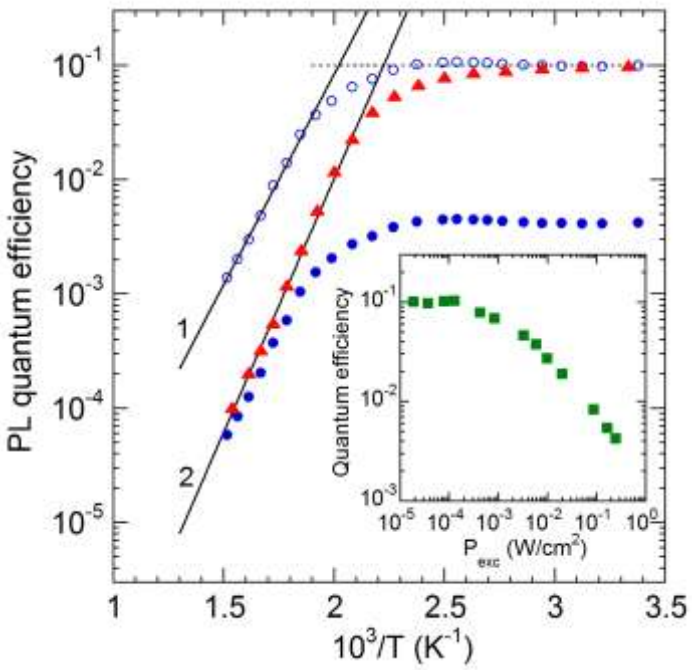

Figure 12. Temperature dependence of YL1 intensity in undoped GaN (sample svt750 grown by MBE). The filled triangles and circles are the $I^{PL}(T)$ dependences at P_{exc} = 10^{-4} and 0.25 W/cm^2, respectively. The empty circles show the $I^{PL}(T)$ dependence for P_{exc} = 0.25 W/cm^2 shifted vertically to match the low-temperature part of the dependence at P_{exc} = 10^{-4} W/cm^2. The lines 1 and 2 show dependences $A\cdot\exp(E_A/kT)$ with E_A = 730 and 880 meV, respectively. T_0 is 450 and 500 K for the dependences at P_{exc} = 10^{-4} and 0.25 W/cm^2, respectively. The inset shows the dependence of the YL1 quantum efficiency on the excitation intensity.

phenomenon can be understood in the frame of the advanced model, according to which G decreases inside a semiconductor as $\exp(-\alpha x)$ from the sample surface. Indeed, while PL from layers closer to the surface is already saturated at certain excitation intensity, PL from deeper layers would saturate only at higher P_{exc}. Because of this, the transition to the quenching region stretches, and it may not be possible to reach temperatures when PL in all layers are saturated and the slope becomes equal to that obtained at very low P_{exc}. High excitation intensity (P_{exc} = 20 W/cm^2) in Ref. [64] may be the reason why the quenching of the yellow band in undoped GaN begins at T > 500 K and the intensity decreases by less than two orders of magnitude before 700 K, with apparent E_A = 650 meV (see the Appendix). On the other hand, in the semi-insulating

GaN:C sample the quenching may be abrupt and tunable (Section 2.3). The transition at $T \approx T_0$ may be blurred due to several reasons, so that the apparent slope is sample-dependent.[9] Unfortunately, the authors of Ref. [64] have not checked if the quenching dependence changes with excitation intensity. But in any case, based on above analysis, we question the attribution of the yellow band in GaN to two types of defects.

High excitation intensity may also cause an artificial rise of PL intensity with temperature. An example is the RL2 band with a maximum at 1.7-1.8 eV in undoped GaN, which is presumably caused by a native defect or a complex, most likely a deep donor with two excited states. The RL2 lifetime is very long at low temperatures (100-150 μs at 15 K), and it decreases significantly with increasing temperature (~2 μs at 100 K).[11] When steady-state PL measurements are conducted at insufficiently low excitation intensity, the PL intensity is saturated at low temperature but not saturated at elevated temperatures, so that the measured PL intensity increases with increasing temperature.[65] When the experiment is conducted at very low excitation intensity to avoid the saturation, no increase in the RL2 intensity is observed.[11] It is likely that the red luminescence band in MBE-grown GaN studied by Hoffmann *et al*.[66] is the RL2 band, and the observed rise in the $I^{PL}(T)$ dependence is also caused by too high excitation intensity.

3.3.2. Photoluminescence in Heavily Doped Semiconductors

In high-quality GaN samples (*n*-type, nondegenerate, with relatively low density of structural defects), the quenching of the YL1 band (when measured at low P_{exc}) begins at about 450 K and reveals E_A = 0.8-0.9 eV (Figure 1).[11,14,30,37] The slope of the quenching may be notably larger

for semi-insulating samples (Figure 4). Note that the actual slope of the abrupt quenching may be sample-dependent (Section 3.3.3).[9]

For samples with high concentration of defects, a transition from the temperature-independent region to the exponential decrease may be smoothened, and the measured slope is smaller in this case. Examples include *n*-type GaN co-doped with Si and C (**Figures** 10 and **13**) and degenerate *n*-type GaN samples doped with Si ($n \approx 10^{19}$ cm^{-3}) or co-doped with Si and Zn (Figure 9).[52,67] Note that in all these samples the YL1 band maximum shifts with variation of excitation intensity (by up to ~100 meV), much more than it may shift due to the DAP nature of transitions (up to ~8 meV).[67] This can be explained by potential fluctuations caused by random distribution of charged defects.[67,68] In this case, diagonal transitions between spatially separated electrons and holes cause the broadening of a PL band and a wide range of PL lifetimes due to a wide range of separations. Figure 13 illustrates how the smoothening of the $I^{PL}(T)$ dependence can

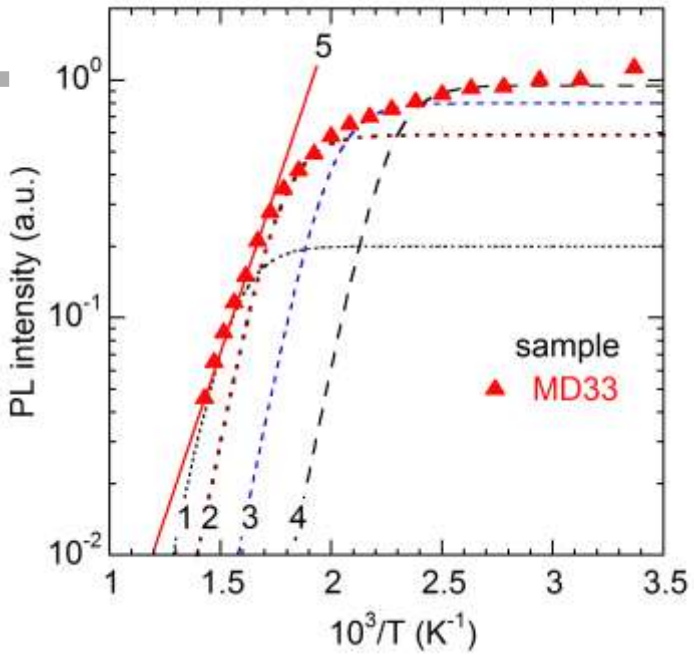

Figure 13. Temperature dependence of YL1 intensity in GaN co-doped with Si and C (sample MD33 grown by MOCVD). The line 5 is the dependence $C^{-1}\exp(E_A/kT)$ with C

= 2×10^5 and E_A = 0.55 eV. The lines 1-4 are calculated using Equations (1) and (3) with the following parameters: E_A = 0.84 eV, C_{pA} = 3×10^{-7} cm^3/s, and different values of τ_{i0}: 1 μs (curve 1), 10 μs (2), 100 μs (3), and 1 ms (4). Reprinted from [M. A. Reshchikov "Giant shifts of photoluminescence bands in GaN", J. Appl. Phys. **2020**, 127, 055701], with the permission of AIP Publishing.

be explained. PL from electron-hole pairs with larger separation (longer τ_{i0}) is quenched at lower temperature than PL from pairs with smaller separation (shorter τ_{i0}). Although the activation energy for all pairs is the same (0.8-0.9 eV), the measured PL intensity from all pairs would reveal a smaller slope.

3.3.3. "Activation Energy" in Tunable Quenching

In classic version of the abrupt and tunable quenching model,[9] the PL quenching is caused by a transition from the population inversion statistics to the equilibrium statistics in a narrow range of temperatures. For PL in Zn-doped GaN, the calculated slope of this transition corresponds to $E_A \approx 5$ eV.[9] In experiments, the apparent E_A varies between 0.6 and 1.0 eV for different GaN:Zn samples. The reduction in the slope and the scatter in the value of E_A were attributed to blurring due to the exponential decrease of incident light intensity with depth, the competition between several types of nonradiative defects, and the presence of potential fluctuations in high-resistivity semiconductors that occur due to random distribution of charged defects.[9]

The PL intensity may abruptly drop by four orders of magnitude at T_0 in semi-insulating GaN doped with Zn or C if the dominant nonradiative center is a deep donor.[9,37] For shallower acceptors (such as Mg_{Ga}), or when the nonradiative center is a deep acceptor, the drop may be notably smaller or not observed at all. Analysis of rate equations for a model with three types of defects [9] shows that for some parameters the PL is tunable but not abrupt. Instead, a slope is observed which corresponds to the ionization energy of the radiative acceptor. An example is shown in **Figure 14**. When the nonradiative center is a deep donor, and $N_S > N_A > N_D$, i.e. the

semiconductor is a high-resistivity *n*-type, the abrupt and tunable quenching occurs at T_0, whereas at $T > T_0$, after the drop, the PL intensity decreases as $\exp(E_A/kT)$ with E_A being the acceptor ionization energy.[9] The magnitude of the drop R decreases with decreasing E_A, so that the abrupt drop can barely be noticed at small E_A (Figure 14a). At the same time, the quenching is tunable, as can be seen from Figure 14b.

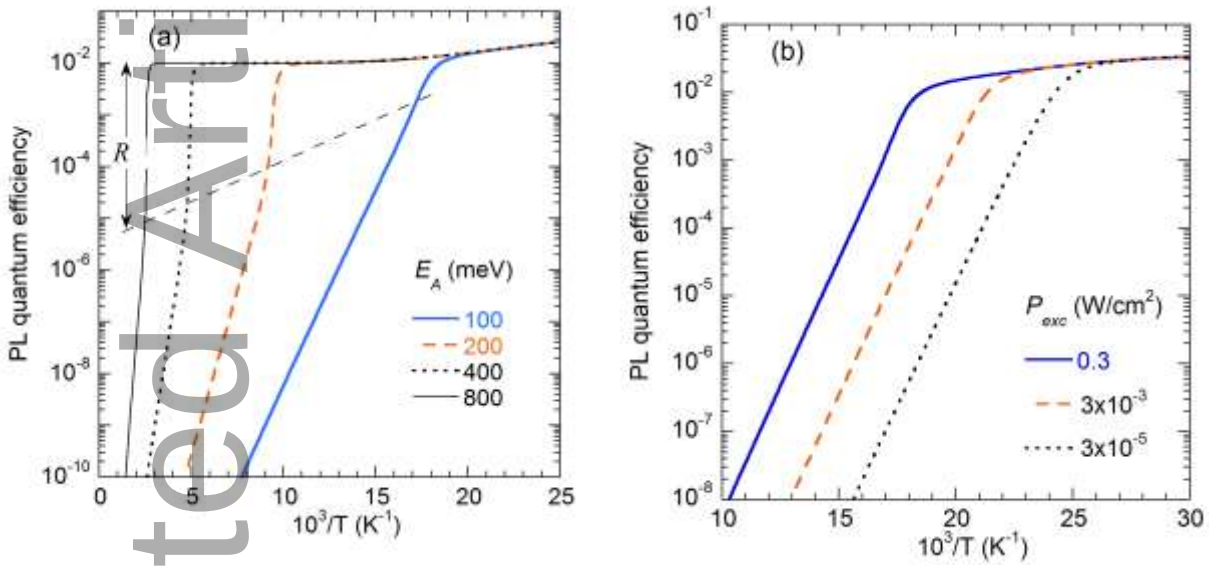

Figure 14. The $\eta(T)$ dependences calculated for a semiconductor with three types of defects (D, A, and S) with S being a deep nonradiative donor.[9] The thin dashed line in (a) shows how the magnitude of the abrupt drop R changes with E_A. The following parameters are used in the calculations: $N_S = 10^{19}$, $N_A = 10^{18}$, $N_D = 10^{17}$ (all in cm^{-3}); $C_{nS} = C_{pS} = C_{pA} = 10^{-6}$, $C_{nD} = 10^{-7}$, $C_{nA} = C_{DA} = 10^{-12}$ (all in cm^3/s); $E_D = 30$ meV. In (a) E_A is varied from 100 to 800 meV and $P_{exc} = 0.3$ W/cm^2. In (b) P_{exc} is varied from 3×10^{-5} to 0.3 W/cm^2 and $E_A = 100$ meV.

3.3.4. Other Reasons for Deviations in the Activation Energy of Quenching

In addition to the cases considered above, the $I^{PL}(T)$ dependence can be affected by several other reasons. One of them is the temperature dependence of the effective density of states in the valence band ($N_V \propto T^{3/2}$). At $T < T_0$, the term with N_V in Equations (1) and (3) can be ignored. At $T > T_0$, the $N_V(T)$ dependence results in a slight increase of the quenching slope. For example, the $I^{PL}(T)$ dependence for the YL1 band reveals $E_A = 880$ meV when the experimental data are fitted

using Equation (1) with a constant parameter C and E_A = 840 meV with C given by Equation (3) with $N_V \propto T^{3/2}$.

The experiments with changing temperature should be carefully designed to avoid artificial changes in the $I^{PL}(T)$ dependences. For example, the $I^{PL}(T)$ dependence shown in **Figure 15** has a slope corresponding to E_A = 890 meV when T increases from 300 to 700 K during 3 hours, and E_A = 790 meV for the subsequent cooling down the sample. The overall decrease in the PL intensity is permanent, and it may be caused by photo-induced reactions at the sample surface or in the bulk, facilitated by high temperatures. Heating to lower temperatures results in less changes and more reproducible dependences. This effect is also sample-dependent.

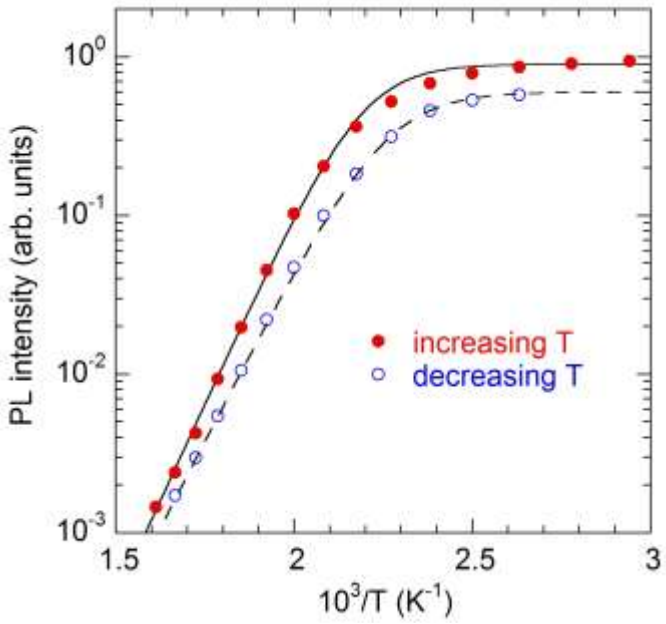

Figure 15. Temperature dependence of YL1 intensity in undoped GaN grown by MBE. The temperature was raised from 300 to 700 K and then decreased to 380 K. The lines are calculated using Equations (1) and (3) with τ_{i0} = 500 μs (obtained from time-resolved PL) and the following fitting parameters: E_A = 890 meV and C_{pA} = 1×10^{-6} cm^3/s for increasing T and E_A = 790 meV and C_{pA} = 1.5×10^{-7} cm^3/s for decreasing T.

Finally, the E_A may be incorrectly found from valid experimental data. An example is E_A = 56±1.5 meV for the YL1 band in undoped GaN reported in [69]. From analysis of PL spectra taken at different temperatures (from 300 to ~600 K),[69] the E_A can be estimated as 0.8-0.9 eV by fitting with Equation (1). However, the authors of that work, instead of the $I^{PL}(T)$ dependence, analyzed the slope of the $I^{PL}(0)– I^{PL}(T)$ dependence at $T > T_0$, where $I^{PL}(0)$ was PL intensity at T = 300 K.

4. Thermal Quenching of Photoluminescence in Other Materials

4.1. Alkali Halides

F-centers in alkali halides were in the focus of early research on point defects in solids.[70] The F-center is an anionic vacancy, such as V_{Cl}, in KCl or NaCl. Because of very wide bandgaps in alkali halides (6-11 eV), defect-related PL was usually excited with below-bandgap light, from the ground state to an excited state of the defect (transition 1′ in Figure 1). As an example, for KCl with $E_g \approx 8.7$ eV, the maximum of the PL excitation band is observed at 2.3 eV, and the PL maximum (transition 3) is observed at 1.2 eV. The ground state of the F-centers is a very deep donor state, while the excited state is shallow, located at $\Delta E \approx 0.1$ eV below the conduction band (0.15 eV for KCl).[70,71] Thermal emission of electrons from the excited state to the conduction band is responsible for the quenching of PL from F-centers.[70,72] Both PL intensity and PL lifetime in KCl decrease above $T \approx 100$ K, and the dependences can be described using Equation (1) with $C \approx 7\times10^5$ and $E_A = \Delta E \approx 0.15$ eV.[72,73] This quenching is explained by thermal emission of electrons from the excited state to the conduction band and their recombination via a nonradiative channel.[70] Note that in nearly all studies on F-centers in alkali halides PL was excited resonantly, so that no holes were produced in the valence band. Then the internal

quantum efficiency can reach 100% if the barrier for the nonradiative path (E_2 in Figure 1) is sufficiently high (0.6 eV for KCl).[70] Photoconductivity also increases exponentially, simultaneously with the PL quenching, in agreement with suggested mechanism of the thermal quenching.[74] When PL in KCl is excited with above-bandgap light, a PL band with a maximum at 2.9 eV is observed.[75] Timusk and Martienssen [75] attributed this band to a radiative transition from the ground state of the F-center to the valence band, assuming that both transitions via the F-center are radiative (they were not able to measure PL spectrum at photon energies lower than 2 eV).

The Seitz-Mott mechanism of thermal quenching was proposed for the Tl-related luminescence with a PL maximum at 4.1 eV and absorption maximum at 5.0 eV in Tl-doped KCl.[76] The PL quenching with $E_A \approx 0.60$ eV was explained as a nonradiative transition of electrons from the excited state to the ground state over a barrier (transition 4 in Figure 1).[76,77] The excited state was predicted to be located very deep in the gap.[78] However, for F-centers in alkali halides this mechanism is unlikely, because the excited state is located close to the conduction band, and electrons escape via the conduction band to other defects at temperatures well below those required for overcoming a barrier in the Seitz-Mott mechanism.

4.2. II-VI Compounds

Along with alkali halides, II-VI semiconductors, such as ZnS, CdS (often called phosphors) were very popular in early research into optical properties of defects in solids. Luminescence from the phosphors was used in radars and TV screens, and thermal quenching of the luminescence attracted significant attention. In some cases, the PL quenching in II-VI phosphors was explained with the Seitz-Mott mechanism,[79] and in others by the Schön-Klasens mechanism.[80] However,

because of poor understanding of defects and insufficient purity of these materials, the early explanations were not convincing and the results casted doubt. In rare cases the Schön-Klasens mechanism has been confirmed by a comparison of the E_A found from Equation (1) and the ionization energy calculated from the energy position of the ZPL in the low-temperature PL spectrum.[81]

In the early stage of PL studies, it was commonly assumed that impurities are needed as activators to produce PL. Prener and Williams [82] proposed a model of activator-coactivator system. According to this model, activators (acceptor impurities) and coactivators (donor impurities) in the nearest-neighbor sites serve as an efficient radiative recombination channel (the so-called associated DAPs). Later, the same authors introduced a concept of self-activated PL, where a cation vacancy in II-VI semiconductors acted as an acceptor in samples doped with shallow donors.[83] The model was further developed by Koda and Shionoya [84,85] and applied to several defects in ZnS. In particular, the "self-activated" band with a maximum at 2.6 eV in Cl-doped ZnS has been attributed to the $V_{Zn}Cl_S$ complex. The thermal quenching of this PL band above T = 220 K was explained with the Schön-Klasens mechanism, and the activation energy E_A = 0.64 eV was attributed to the thermal depth of the acceptor ground state from the valence band.[84] At that time Shionoya *et al.*[85] emphasized that two localized states (ground and excited) are necessary in order to apply the configuration coordinate model, similar to the case of F-centers in alkali halides. The excited and ground states corresponded to the donor and acceptor states of the associated pair. Note that the quenching of PL from localized defects, to which the configuration coordinate model could be applied, was usually explained by the Seitz-Mott mechanism,[1] with a few exceptions.

Similar to self-activated luminescence in ZnS, the dominant PL band at ~1.45 eV in *n*-type CdTe (E_g = 1.60 eV) was attributed to the $V_{Cd}D$ complexes (also called the A centers).[86,87] In particular, a DAP-type PL band with a maximum at 1.444 eV and the NBE peak at 1.581 eV in I-doped CdTe is quenched at T > 100 K with E_A = 125 meV, and this quenching was attributed to thermal emission of holes from the $V_{Cd}I_{Te}$ acceptor to the valence band.[86] Similar results were obtained for the 1.45 eV band in CdTe doped with In or Br. The thermal quenching with E_A = 95 meV was attributed to ionization of the $V_{Cd}In_{Cd}$ and $V_{Cd}Br_{Te}$ acceptors via the Schön-Klasens mechanism.[87] The DAP-type nature of this PL was confirmed with time-resolved PL experiments, where nonexponential decay was observed after a laser pulse at T = 5 K. These results are similar to classic cases of PL quenching in *n*-type GaN (Section 2.1). In addition to the main quenching, a slow decrease of PL intensity before the PL quenching in *n*-type CdTe was attributed to thermal emission of electrons from shallow donors to the conduction band.[86,87] However, this reason is unlikely, because the decrease was also observed in degenerate samples, and there are other explanations for slow changes in PL intensity (Section 3.3).

The tunable by excitation intensity PL quenching was observed from ZnS powder doped with Ag and Co.[33] Klasens,[88,89] by analyzing possible solutions of rate equations derived within a model that included radiative and nonradiative defects, concluded that tunable quenching is possible for certain parameters of the model. Maeda [90] investigated PL from conductive and insulating CdS samples. While in the former the PL quenching was “normal” (i.e., by the Schön-Klasens mechanism), an unusual quenching behavior (tunable by excitation intensity) has been observed for the insulating sample, in agreement with the mechanism of abrupt and tunable quenching (Section 2.3).[2]

4.3. III-V Compounds

Besides GaN and other III-nitrides, PL was extensively studied in GaAs and GaP.[91,92] The dominant defect-related PL band in *n*-type GaAs is the 1.2 eV band, the so-called "self-activated" band attributed to the $V_{Ga}D$ complex, where D is a shallow donor (such as Te_{As} or Sn_{Ga}).[93] Williams [93] explained the PL quenching with the Seitz-Mott mechanism (**Figure 16**) and found E_A = 0.18 eV. Note that the samples were degenerate ($n > 10^{18}$ cm^{-3} at T = 77 K), so that, with today's knowledge, transitions of electrons from the conduction band to the acceptor level would be proposed for this emission.

Later, it became clear that the quenching of the 1.2 eV band is caused by ionization of the $V_{Ga}D$ acceptors, i.e. by the Schön-Klasens mechanism, and $E_A \approx$ 0.15-0.18 eV is the ionization energy of these acceptors.[94,95] The crucial evidence for such attribution in those works was the observation of a simultaneous rise in the NBE emission in samples with the internal quantum efficiency of the 1.2 eV band close to unity (Section 3.2.1).

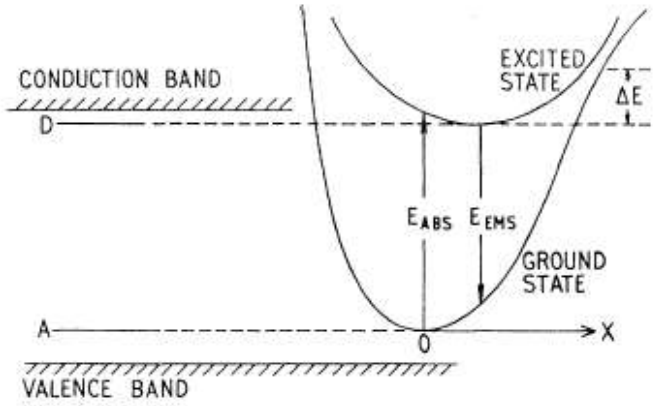

Figure 16. The band diagram and the configuration coordinate model of the self-activated luminescence in GaAs. The quenching of the 1.2 eV band is explained by nonradiative transitions over the barrier *ΔE*. Reprinted with permission from [E. W. Williams, "Evidence for Self-Activated Luminescence in GaAs: The Gallium Vacancy-Donor Center", Phys. Rev. **168**, 922 (1968)], Copyright © 1968 by the American Physical Society.

In a similar manner, Hwang [96] explained the temperature dependence of the 1.37 eV band in *p*-type GaAs doped with Cd or Zn. This PL band was attributed to the AV_N complexes with A = Cd_{Ga} or Zn_{Ga}. The quenching of the 1.37 eV band with E_A = 0.087 eV was explained with the Seitz-Mott mechanism, where E_A = 0.087 eV is the barrier height for a nonradiative transition from the excited state to the ground state of the associated pair. It seems more reasonable to attribute the PL quenching to thermal emission of electrons from a donor located at ~0.09 eV to the conduction band, i.e. to the Schön-Klasens mechanism. The shape of the 1.37 eV band with FWHM ≈ 0.1 eV is asymmetric, so that the ZPL can be predicted at about 1.40-1.42 eV. This is consistent with the threshold at ~1.45 eV for the resonant excitation of the PL. Since the bandgap of GaAs is 1.52 eV at low temperatures, the sum of the donor and acceptor ionization energies can be found as 0.10-0.12 eV, and the 1.37 eV band can be attributed to the DAP-type transitions with the Zn_{Ga} and Cd_{Ga} acceptors having the ionization energies of 0.031 and 0.035 eV, respectively.[92] Interestingly, Hwang [96] rejected the Schön-Klasens mechanism on the grounds that the quenching of the 1.37 eV band was not accompanied by a rise in the NBE emission. However, as it was discussed in Section 3.2.1, the simultaneous with the quenching rise in other PL bands can be observed only when the internal quantum efficiency of the dominant PL band is very high, what probably was not the case for *p*-type GaAs:Zn and GaAs:Cd samples.

In another work, the value of E_A ≈ 0.077 eV was obtained from the slope of quenching of the Cu-related 1.216 eV band with FWHM = 0.13 eV in Cu-diffused *p*-type InP samples (E_g = 1.425 eV).[97] Note that the E_A might be underestimated in this work, because the transition from the temperature-independent part to the exponential decrease stretched from 20 K to 70 K, and the slope was analyzed in a small temperature range where PL intensity decreased by only one order

of magnitude. The $E_A \approx 0.077$ eV was attributed to a barrier between the excited and ground state (Seitz-Mott mechanism),[97] whereas the DAP model and thermal emission of photogenerated electrons from the Cu-related donor to the conduction band (Schön-Klasens mechanism) would be a more reasonable explanation.

Maeda [98] observed two-step tunable quenching for the DAP luminescence in GaP, the behavior similar to the one reported for Zn-doped GaN.[40] From the $T_0(G)$ dependence, $E_A \approx$ 0.09 eV and other reasonable parameters could be obtained by using Equation (4).[2] The quenching in that work is tunable but not abrupt, which could be related to specific parameters of nonradiative centers in the studied material as discussed in Section 3.3.3.

5. Conclusion

Thermal quenching of PL in semiconductors reveals critical properties of the material and parameters of defects introduced intentionally (by doping) or unintentionally. Rate equations models successfully describe temperature dependence of defect-related luminescence. The Schön-Klasens mechanism is the main mechanism of PL quenching in semiconductors. It attributes the quenching to a thermal emission of photogenerated charge carriers from a defect level to the free band and subsequent recombination via nonradiative channels. The activation energy of the quenching reveals the defect ionization energy in this case. In semi-insulating materials, the abrupt and tunable quenching of PL is often observed. According to this mechanism, the slope of the thermal quenching in the Arrhenius plot may be independent of any ionization or activation energy and is extremely high in some cases. Finally, the quenching with the Seitz-Mott mechanism (conversion of radiative recombination into nonradiative

recombination via the same defect with increasing temperature) is rare or nonexistent in semiconductors.

6. Experimental details

GaN samples analyzed in this work were grown by MBE (at VCU), MOCVD (at TUBS and University of Magdeburg, Germany) and HVPE (Kyma Technologies, TDI and Nitride Crystals) methods on c-plane sapphire substrates. Other details can be found in the cited works. Steady-state and time resolved PL was excited with a HeCd and pulsed nitrogen lasers, respectively. Other details can be found elsewhere.[30] It is important to mention that the spectra shown in this work may be slightly different from those reported in the literature and even from the spectra in our own works. The reason is that beginning with Ref [30], for convenience of comparison with theoretically predicted PL band shapes, we present PL spectra as the number of emitted photons in relative units plotted as a function of photon energy. For this, the originally measured $I^{PL}(\lambda)$ dependences, after correction for the spectral response of the measurement system, are multiplied by λ^3.[30,99]

Acknowledgements

The author wishes to thank J. Leach (Kyma Technologies, Inc.), A. Usikov (with TDI, Inc. and now with Nitride Crystals, Inc.), A. Waag (TUBS, Germany), A. Strittmatter (University of Magdeburg, Germany), and H. Morkoç (VCU) for providing GaN samples analyzed in this work. The work was supported by the National Science Foundation (DMR-1904861).

Conflict of Interest

The author declares no conflict of interest.

Keywords

photoluminescence, quenching, semiconductors, GaN, F-centers, tunable quenching

Appendix

An expression for the $\eta(T)$ dependence for PL from defects in *n*-type semiconductors has been derived previously in the limit of low excitation intensity.[9,14] Below this dependence is generalized for the case of arbitrary excitation intensity. Let us consider an *n*-type semiconductor with shallow donors (the concentration N_D), radiative acceptors (N_A), and nonradiative centers (N_S). The electron- and hole-capture coefficients for these defects are C_{ni} and C_{pi}, respectively, where $i = D$, A, and S. The concentration of free electrons n is constant (in nondegenerate samples at relatively high temperatures when majority of shallow donors are ionized or in degenerate samples at any temperature). We also assume that the nonradiative centers cannot be saturated with photogenerated carriers because of fast capture and recombination, and the nonradiative channel is not quenched since the defect level is very deep. Band-to-band recombination can also play the role of the S channel. We will explore how an increase in the excitation intensity, P_{exc}, affects the $\eta(T)$ dependence. Electron transitions for this case are shown in the inset to Figure A1.

The rate equation involving transitions to and from the conduction band in steady state is

$$G = \frac{N_A^0}{\tau_0} + \frac{N_S^0}{\tau_S}, \quad \text{(A1)}$$

where G is the electron-hole generation rate, $\tau_0 = (C_{nA} n)^{-1}$, $\tau_S = (C_{nS} n)^{-1}$ are the characteristic times of transitions 1 and 2, respectively, and N_A^0 and N_S^0 are the concentrations of the A and S centers filled with holes in steady state. The rate equation involving transitions to and from the valence band is

$$G = C_{pA}(N_A - N_A^0)\, p - \frac{N_A^0}{\tau_{therm}} + C_{pS} N_S\, p \quad \text{(A2)}$$

with

$$\tau_{therm} = \frac{g \exp\left(\frac{E_A}{kT}\right)}{C_{pA} N_V},$$

where p is the steady-state concentration of holes in the valence band, and τ_{therm} is the characteristic time of thermal emission of holes from acceptor A to the valence band. The rate equation involving transitions to and from the acceptor A is

$$C_{pA}(N_A - N_A^0)\, p = \frac{N_A^0}{\tau_{therm}} + \frac{N_A^0}{\tau_0}. \quad \text{(A3)}$$

At low temperature (below the thermal quenching) and at low excitation intensity (to avoid saturation of defects with holes), the internal quantum efficiency of transitions via A center is

$$\eta_0 = \frac{C_{pA} N_A}{C_{pA} N_A + C_{pS} N_S}. \quad \text{(A4)}$$

From Equations (A1)-(A4), N_A^0 can be found. Then, the temperature dependence of the PL efficiency (transition 1), is

$$\eta(G,T) = \frac{N_A^0}{\tau_0 G} = \frac{B}{2} - \sqrt{\frac{B^2}{4} - C}\,, \qquad \text{(A5)}$$

where $B = 1 + \frac{C}{\eta_0}\left[1 + \frac{\tau_0(1-\eta_0)}{\tau_{therm}}\right]$ and $C = \frac{N_A}{G\tau_0}$.

At low excitation intensity, at $G << G_{cr} = N_A(\eta_0\tau_0)^{-1}$, Equation (A5) becomes

$$\eta(T) = \frac{\eta_0}{1 + \frac{\tau_0(1-\eta_0)}{\tau_{therm}}}. \qquad \text{(A6)}$$

Figure A1 shows the $\eta(T)$ dependences calculated with Equation (A5) for P_{exc} from 10^{-3} to 10 W/cm^2. In these calculations, $G = P_{exc}\alpha/\hbar\omega$, where $\hbar\omega$ is the photon energy of the excitation light and α is the absorption coefficient (α = 1.2×10^5 cm^{-1} at $\hbar\omega$ = 3.81 eV). The T_0 increases with increasing P_{exc} above $G = G_{cr}$, because PL saturates at $T < T_0$ for $G > G_{cr}$, and does not at $T > T_0$. The parameters of the model are close to the parameters reported in Ref. [64] for the undoped GaN sample, and the $\eta(T)$ dependence from that work (in arbitrary units) is shown with empty circles. The slope corresponding to E_A = 650 meV was observed between 570 and 700 K. The results of numerical solution of Equations (A1)-(A4) within the model accounting for the exponential decrease of the excitation light intensity inside the semiconductor are shown with crosses. The $\eta(T)$ dependence is rounded near T_0 and the slope is reduced between 570 and 700 K because of a gradual saturation of PL in layers located farther from the sample surface.

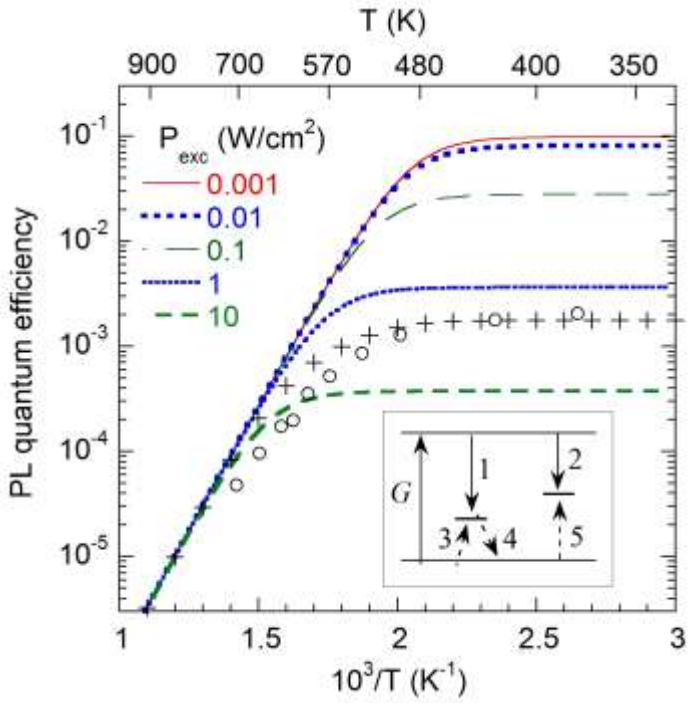

Figure A1. The $\eta(T)$ dependences calculated using Equation (A5) with the following parameters: $N_A = 6\times10^{16}$ cm^{-3}, $C_{pA} = 4\times10^{-7}$ cm^3/s, $C_{nA} = 1.1\times10^{-13}$ cm^3/s, $n = 8\times10^{16}$ cm^{-3}, $\eta_0 = 0.1$, $E_A = 850$ meV, and different P_{exc}. The crosses show numerical solutions of Equations (A1)-(A4) in assumption that $G(x) = P_{exc}\alpha \exp(-\alpha x)/\hbar\omega$ with $P_{exc} = 20$ W/cm^2. Empty circles are the experimental points for the undoped GaN studied in [64]. The inset shows a band diagram with electron (solid arrows) and hole (dashed arrows) transitions via radiative acceptor A and nonradiative center S.

The intensity of defect-related photoluminescence (PL) in semiconductors decreases exponentially above some critical temperature, a process called the PL quenching. Here, main mechanisms of PL quenching, including Schön-Klasens mechanism, abrupt and tunable quenching, and "negative" thermal quenching are reviewed. Examples are given for major defects in GaN and a few iconic cases previously analyzed in I-VII, II-VI and III-V compounds.

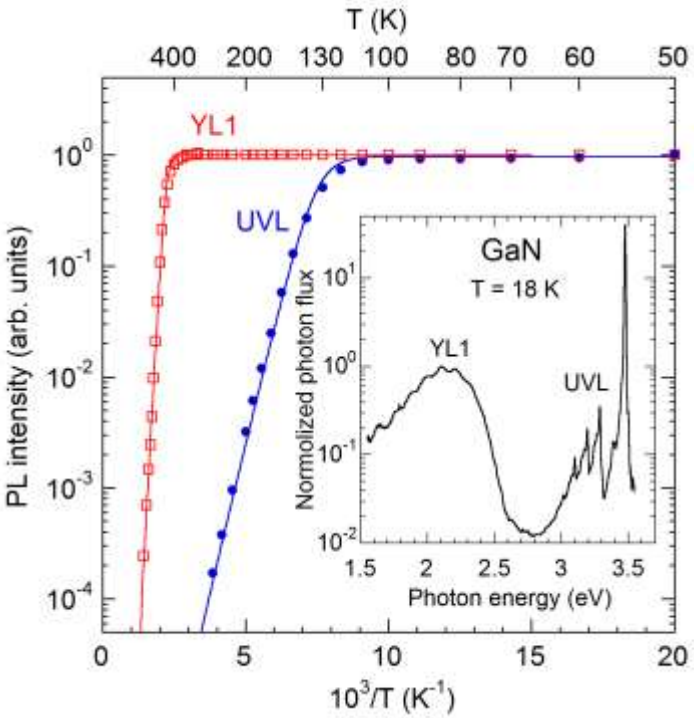

Keyword: photoluminescence
s

References

[1] S. Shionoya, "Photoluminescence", in *Luminescence of Solids*, ed. by. D. R. Vij, Plenum Press, New York, USA **1998**, pp. 95-133.

[2] M. A. Reshchikov, *J. Appl. Phys*. **2014**, 115, 012010.

[3] F. Seitz, *Trans. Faraday Soc*. **1939**, 35, 74.

[4] R. W. Gurney and N. F. Mott, *Trans. Faraday Soc*. **1939**, 35, 69.

[5] A. M. Stoneham, *Theory of Defects in Solids*, Clarendon Press, Oxford, **2001**. pp. 291-317.

[6] C. C. Klick and J. H. Schulman [in *Solid State Physics*, edited by F. Seitz and D. Turnbull (Academic Press Inc., New York, **1957**), Vol. 5, p. 97].

[7] M. Schön, *Z. Phys*. **1942**, 119, 463.

[8] H. A. Klasens, *Nature* **1946**, 158, 306.

[9] M. A. Reshchikov, A. A. Kvasov, M. F. Bishop, T. McMullen, A. Usikov, V. Soukhoveev, and V. A. Dmitriev, *Phys. Rev. B* **2011**, 84, 075212.

[10] H. Morkoç, *Handbook of Nitride Semiconductors and Devices*, Wiley Press, **2008**.

[11] M. A. Reshchikov and H. Morkoç, *J. Appl. Phys*. **2005**, 97, 061301.

[12] D. G. Thomas, J. J. Hopfield, and W. M. Augustyniak, *Phys. Rev*. **1965**, 140, A202.

[13] M. A. Reshchikov, J. D. McNamara, F. Zhang, M. Monavarian, A. Usikov, H. Helava, Yu. Makarov, and H. Morkoç, *Phys. Rev. B* **2016**, 94, 035201.

[14] M. A. Reshchikov and R. Y. Korotkov, *Phys. Rev. B* **2001**, 64, 115205.

[15] M. A. Reshchikov, J. D. McNamara, M. Toporkov, V. Avrutin, H. Morkoç, A. Usikov, H. Helava, and Yu. Makarov, Scientific Reports **2016**, 6, 37511.

[16] E. R. Glaser, M. Murthy, J. A. Freitas, Jr., D. F. Storm, L. Zhou, and D. J. Smith, *Physica B* **2007**, 401-402, 327.

[17] M. A. Reshchikov, P. Ghimire, and D. O. Demchenko, *Phys. Rev. B* **2018**, 97, 205204.

[18] A. Hangleiter, J. S. Im, T. Forner, V. Harle, and F. Scholz, *Mater. Res. Soc. Symp. Proc*. **1996**, 395, 559.

[19] T. Malinauskas, K. Jarašiūnas, R. Aleksiejunas, D. Gogova, B. Monemar, B. Beaumont, and P. Gibart, *Phys. Stat. Sol.* (*b*) **2006**, 243, 1426.

[20] A. Dmitriev and A. Oruzheinikov, *J. Appl. Phys*. **1999**, 86, 3241.

[21] L. Eckey, V. von Gfug, J. Holst, A. Hoffmann, A. Kaschner, H. Siegle, C. Thomsen, B. Schineller, K. Heime, M. Heuken, O. Schön, and R. Beccard, *J. Appl. Phys*. **1998**, 84, 5828.

[22] U. Kaufmann, M. Kunzer, M. Maier, H. Obloh, A. Ramakrishnan, and B. Santic, *Appl. Phys. Lett.* **1998**, 72, 1326.

[23] M. A. Reshchikov, G.-C. Yi, and B. W. Wessels, *Phys. Rev. B* **1999**, 59, 13176.

[24] F. Shahedipour and B. W. Wessels, *Appl. Phys. Lett*. **2000**, 76, 3011.

[25] F. Shahedipour and B. W. Wessels, *MRS Internet Journal of Nitride Semicond. Res*. **2001**, 6, 12.

[26] M. Godlewski, T. Suski, I. Grzegory, S. Porowski, J. P. Bergman, W. M. Chen, and B. Monemar, *Physica B* **1999**, 273-274, 39.

[27] B. Han, J. M. Gregie, and B. W. Wessels, *Phys. Rev. B* **2003**, 68, 045205.

[28] E. Malguth, A. Hoffmann, W. Gehlhoff, O. Gelhausen, M. R. Phillips, X. Xu, *Phys. Rev. B* **2006**, 74, 165202.

[29] E. Richter, E. Gridneva, M. Weyers, and G. Tränkle, *J. Cryst. Growth* **2016**, 456, 97.

[30] M. A. Reshchikov, M. Vorobiov, D. O. Demchenko, Ü. Özgür, H. Morkoç, A. Lesnik, M. P. Hoffmann, F. Hörich, A. Dadgar, and A. Strittmatter, *Phys. Rev. B* **2018**, 98, 125207.

[31] M. Iwinska, R. Piotrzkowski, E. Litwin-Staszewska, T. Sochacki, M. Amilusik, M. Fijakowski, B. Lucznik, and M. Bockowski, *Appl. Phys. Express* **2017**, 10, 011003.

[32] N. R. Nail, F. Urbach, and D. Pearlman, *J. Optical Soc. Amer*. **1949**, 39, 690.

[33] C. G. Hill and H. A. Klasens, *J. Electrochem. Soc*. **1949**, 96, 275.

[34] M. A. Reshchikov, *AIP Conf. Proc.* **2014**, 1583, 292. Doi: 10.1063/1.4865655.

[35] Weak temperature dependence of N_V causes a small overestimate in E_A, but it can be ignored in the first approximation.

[36] M. A. Reshchikov, J. McNamara, S. Fernandez, and R. Calarco, *Phys. Rev. B* **2013**, 87, 115205.

[37] M. A. Reshchikov, N. M. Albarakati, M. Monavarian, V. Avrutin, and H. Morkoç, *J. Appl. Phys.* **2018**, 123, 161520.

[38] M. Vorobiov, O. Andrieiev, and M. A. Reshchikov, unpublished.

[39] J. D. McNamara, N. M. Albarakati, and M. A. Reshchikov, J. Lumin. **2016**, 178, 301.

[40] M. A. Reshchikov, *Phys. Rev. B* **2012**, 85, 245203.

[41] M. A. Reshchikov, "Photoluminescence from defects in wide-bandgap, direct-gap semiconductors", book chapter in *Characterization and Control of Defects in Semiconductors*, Ed. F. Tuomisto, IET, UK, **2019**, pp. 45-96. ISBN-13: 978-1-78561-655-6.

[42] D. O. Demchenko, I. C. Diallo, and M. A. Reshchikov, *J. Appl. Phys.* **2016**, 119, 035702.

[43] M. A. Reshchikov, D. O. Demchenko, J. D. McNamara, S. Fernández-Garrido, and R. Calarco, *Phys. Rev. B* **2014**, 90, 035207.

[44] M. A. Reshchikov, *J. Appl. Phys*. **2014**, 115, 103503.

[45] M. A. Reshchikov, D. O. Demchenko, A. Usikov, H. Helava, and Yu. Makarov, *Phys. Rev. B*, **2014**, 90, 235203.

[46] M. A. Reshchikov, J. D. McNamara, A. Usikov, H. Helava, and Yu. Makarov, *Phys. Rev. B* **2016**, 93, 081202(R).

[47] M. Lax, *J. Phys. Chem. Solids* **1959**, 8, 66.

[48] A. Alkauskas, M. D. McCluskey, and C. G. Van de Walle, *J. Appl. Phys.* **2016**, 119, 181101.

[49] A. Alkauskas, Q. Yan, and C. G. Van de Walle, *Phys. Rev. B* **2014**, 90, 075202.

[50] D. Wickramaratne, C. E. Dreyer, B. Monserrat, J.-X. Shen, J. L. Lyons, A. Alkauskas, and C. G. Van de Walle, *Appl. Phys. Lett.* **2018**, 113, 192106.

[51] M. A. Reshchikov, M. Foussekis, and A. A. Baski, *J. Appl. Phys.* **2010**, 107, 113535.

[52] M. A. Reshchikov, M. A. Foussekis, J. D. McNamara, A. Behrends, A. Bakin, and A.Waag, *J. Appl. Phys.* **2012**, 111, 073106.

[53] M. A. Reshchikov, X. Gu, J. Nause, and H. Morkoç, *Mat. Res. Soc. Symp. Proc.* **2006**, 892, FF23.11.

[54] M. A. Reshchikov, A. Usikov, H. Helava, Yu. Makarov, V. Prozheeva, I. Makkonen, F. Tuomisto, J. H. Leach, and K. Udwary, Scientific Reports **2017**, 7, 9297.

[55] F. E. Williams and H. Eyring, *J. Chem Phys.* **1941**, 15, 289.

[56] T. Yokogawa, T. Taguchi, S. Fujita, and M. Satoh, *IEEE Trans. Electron. Devices* **1983**, ED-30, 271.

[57] I. Aksenov, M. Matsui, T. Kai, and K. Sato, *Jpn. J. Appl. Phys*. **1993**, 32, 4542.

[58] T. W. Kang, S. H. Park, H. Song, T. W. Kim, G. S. Yoon, and C. O. Kim, *J. Appl. Phys.* **1998**, 84, 2082.

[59] M. Watanabe, M. Sakai, H. Shibata, C. Satou, T. Shibayama, H. Tampo, A. Yamada, K. Matsubara, K. Sakurai, S. Ishizuka, S. Niki, K. Maeda, and I. Niikura, *Physica B* **2006**, 376-377, 711.

[60] H. He, Y. Wang, J. Wang, and Z. Ye, *Phys. Chem. Chem Phys*. **2011**, 13, 14902.

[61] K. Prashanthi, Ž. Antić, G. Thakur, M. D. Dramićanin, and T. Thundat, Phys. Stat. Sol. RRL **2018**, 12, 1700352.

[62] H. Shibata, *Jpn. J. Appl. Phys*. **1998**, 37, 550.

[63] G. Davis, "Optical Measurements of Point Defects", in *Identification of Point Defects in Semiconductors*, *Semiconductors and Semimetals* series, vol. **51B**, Ed. M. Stavola, Acad. Press, **1998**, pp. 49-51.

[64] R. Armitage, W. Hong, G. Yang, H. Feick, J. Gebauer, E. R. Weber, S. Hautakangas, and K. Saarinen, *Appl. Phys. Lett*. **2003**, 82, 3457.

[65] M. A. Reshchikov, M. H. Zhang, J. Cui, P. Visconti, F. Yun, and H. Morkoç, *Mat. Res. Soc. Symp. Proc*. **2001**, 639, G6.7.

[66] D. M. Hofmann, B. K. Meyer, H. Alves, F. Letter, W. Burkhard, N. Romanov, Y. Kim, J. Krüger, and E. R. Weber, *Phys. Stat. Sol.* (*a*) **2000**, 180, 261.

[67] M. A. Reshchikov, *J. Appl. Phys*. **2020**, 127, 055701.

[68] A. P. Levanyuk and V. V. Osipov, *Sov. Phys. Usp*. **1981**, 24, 187.

[69] A. P. Young and L. J. Brillson, *Appl. Phys. Lett*. **2000**, 77, 699.

[70] G. Baldacchini, "Radiative and nonradiative processes in color crystals", in *Advances in Nonradiative Processes in Solids*, Ed. B. Di Bartolo, Plenum Press, New York, **1991**, pp. 219-259.

[71] R. L. Gilbert and J. J. Markham, *J. Chem. Sol.* **1969**, 30, 2699.

[72] S. Honda and M. Tomura, *J. Phys. Soc. Jap.* **1972**, 33, 1003.

[73] L. F. Stiles, Jr., M. P. Fontana, and D. B. Fitchen, *Sol. St. Comm.* **1969**, 7, 681.

[74] R. K. Swank and F. C. Brown, *Phys. Rev*. **1963**, 130, 34.

[75] T. Timusk and W. Martiensen, *Phys. Rev*. **1962**, 128, 1656.

[76] P. D. Johnson and F. E. Williams, *J. Chem. Phys*. **1952**, 20, 124.

[77] F. Seitz, *J. Chem. Phys*. **1938**, 6, 150.

[78] F. E. Williams, *J. Opt. Soc. of Amer*. **1953**, 47, 869.

[79] F. E. Williams, *J. Chem. Phys.* **1947**, 15, 289.

[80] R. H. Bube, *Phys. Rev.* **1953**, 90, 70.

[81] P. J. Dean, B. J. Fitzpatrick, and R. N. Bhargava, *Phys. Rev. B* **1982**, 26, 2016.

[82] J. S. Prener and F. E. Williams, *J. Electrochem. Soc.* **1956**, 103, 342.

[83] J. S. Prener and F. E. Williams, *J. Chem. Sol.* **1956**, 25, 361.

[84] T. Koda and S. Shionoya, *Phys. Rev.* **1964**, 136, A541.

[85] S. Shionoya, T. Koda, K. Era, and H. Fujiwara, *J. Phys. Soc. Jap*. **1964**, 19, 11571167.

[86] J. Lee, N. C. Giles, D. Rajavel, and C. Summers, *J. Appl. Phys*. **1995**, 78, 5669.

[87] W. Stadler, D. M. Hofmann, H. C. Alt, T. Muschik, B. K. Meyer, E. Weigel, G. M. Müller-Vogt, M. Salk, E. Rupp, and K. W. Benz, *Phys. Rev. B* **1995**, 51, 10619.

[88] H. A. Klasens, *J. Phys. Chem. Solids* **1958**, 7, 175.

[89] H. A. Klasens, *J. Phys. Chem. Solids* **1959**, 9, 185.

[90] K. Maeda, *J. Phys. Chem. Solids* **1965**, 26, 1419.

[91] M. Gershenzon, "Radiative recombination in the III-V compounds", in *Semiconductors and Sermimetals*, Ed. R. K. Willardson and A. C. Beer, Vol. **2**: "Physics of III-V Compounds", Acad. Press, New York, **1966**, pp. 289-369.

[92] E. W. Williams and H. B. Bebb, "Photoluminescence II: Gallium Arsenide", in *Semiconductors and Sermimetals*, Ed. R. K. Willardson and A. C. Beer, Vol. **8**: "Transport and Optical Phenomena", Acad. Press, New York, **1972**, pp. 321-392.

[93] E. W. Williams, *Phys. Rev.* **1968**, 168, 922.

[94] K. D. Glinchuk, A. V. Prokhorovich, and V. I. Vorobkalo, *Phys. Stat. Sol.* (*a*) **1976**, 34, 777.

[95] A. A. Gutkin, M. A. Reshchikov, and V. E. Sedov, *Semiconductors* **1997**, 31, 908.

[96] C. J. Hwang, *Phys. Rev*. **1969**, 180, 827.

[97] D. Pal and D. N. Bose, *J. Appl. Phys*. **1995**, 78, 5206.

[98] K. Maeda, *J. Phys. Chem. Solids* **1965**, 26, 595.

[99] I. Pelant and J. Valenta, *Luminescence Spectroscopy of Semiconductors*, Oxford Univ. Press, Oxford, UK, **2012**, p. 61.